Spatial Distribution and Mechanisms of Earthquakes in the Southern New Hebrides Arc From a Temporary Land and Ocean Bottom Seismic Network and From Worldwide Observations

E. Coudert,[1,2,3] B. L. Isacks,[1] M. Barazangi,[1] R. Louat,[2] R. Cardwell,[1] A. Chen,[4] J. Dubois,[2,3] G. Latham,[4] and B. Pontoise[2]

In 1977 a wide-aperture seismic network of land and ocean bottom stations (OBS) was operated for 6 weeks in the southern New Hebrides island arc. Data on the spatial distribution and mechanisms of small events recorded by this local network were integrated with worldwide observations of moderate to large size New Hebrides earthquakes of the past 17 years to study the structure and deformational processes in the New Hebrides subduction zone. Surprisingly, small differences (less than about 10 km) were found between the locations of shallow- and intermediate-depth earthquakes as located by the temporary local network and by the International Seismological Centre using worldwide stations. Analysis of the P wave travel time data from the OBS station closest to the trench shows limited evidence for a high-velocity zone (about 5% higher than the surrounding mantle) associated with the descending plate. The thrust zone between the descending and upper plates is defined mainly by the spatial distribution and focal mechanisms of moderate to large size events and their aftershocks, but it is not very well defined by the spatial distribution of small size events located in this study. Shallow seismic activity located beneath the trench and beneath the interplate thrust zone indicates a lower limit of about 40 km for the thickness of the seismically active part of the descending plate beneath the thrust zone. Focal mechanisms of moderate to large size earthquakes located within the upper plate and geological observations on the islands suggest that the upper plate in the region of Erromango and Tanna is divided into a series of blocks that are differentially uplifted along mainly NW-SE striking faults. During the OBS experiment several shallow events were well located beneath the Coriolis trough, a riftlike feature located to the east of the volcanic arc. Well-determined depths of these events are between 11 and 22 km. The well-located intermediate-depth events define a 20-km-thick Benioff zone that has a dip of about 70°. The spatial distribution of events within the descending slab is very strongly clustered in a persistent pattern that is seen in both the short-term sample of small events determined by the local network and the long-term sample of locations based on worldwide data. Several focal mechanisms of moderate to large size intermediate-depth events show components of lateral extension along the strike of the arc and some show components of lateral compression, both of which could be interpreted as the result of a lateral bending of the descending plate in the part of the southern New Hebrides arc where the trench begins to curve around to the east.

Introduction

The New Hebrides island arc, a subduction zone located in the southwest Pacific, is part of the system of plate boundaries between the Australian and Pacific plates. The evolution of the arc is particularly interesting in respect to its late Cenozoic history of polarity reversal [e.g., *Chase*, 1971; *Karig and Mammerickx*, 1972; *Gill and Gorton*, 1973; *Mallick*, 1975; *Falvey*, 1975; *Carney and MacFarlane*, 1978.]. Since at least Pliocene times the arc has been subducting the oceanic plate of the Coral Sea, and much of the Fiji Plateau may have been created by the southwestward rotation of the arc away from Fiji (see Figure 1). Although the overall geometry of the descending slab beneath the arc seems to be relatively simple, the dip of the slab is quite steep at intermediate focal depths [*Santo*, 1970; *Dubois*, 1971; *Isacks and Molnar*, 1971; *Isacks*

and Barazangi, 1977; *Pascal et al*, 1978; *Isacks et al.*, 1981]. In fact, the New Hebrides Benioff zone has the steepest dip known except possibly for the complex intracontinental Benioff zones beneath the Hindu Kush and Romania.

In this paper we report results of a detailed study of a part of the southern New Hebrides arc, a study based on a uniquely extensive coverage of the arc by a temporary network of seismographs located on islands and on the ocean floor during August and September 1977. To our knowledge, this is the first time that field seismological data have been acquired from land and ocean bottom (OBS) seismic stations that cover more than the total width of an active convergent plate boundary. The network spanned a distance of 350 km across the arc (see Figure 2) and extended from islands located 150 km seaward of the trench to stations in and around the Coriolis trough, a seismically active, riftlike feature [*Dubois et al.*, 1978]. During the 6 weeks of the network's operation, numerous earthquakes were recorded and located in and near the network. Together with published and new data on the larger events recorded by the worldwide network during the preceding 17 years, the results help to define (1) the location and orientation of the plate boundary, (2) the shape, thickness, and stresses within the seismically active part of the subducted plate, and (3) the spatial distribution and mechanisms of earthquakes within the upper plate. Interpretation of the

[1] Department of Geological Sciences, Cornell University, Ithaca, New York 14853.
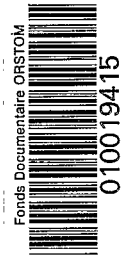
[2] Office de la Recherche Scientifique et Technique Outre Mer, Noumea, New Caledonia.

[3] Laboratoire de Géophysique, Université de Paris 11, 91405 Orsay, France.

[4] Marine Science Institute, Geophysics Laboratory, University of Texas, Galveston, Texas 77550.
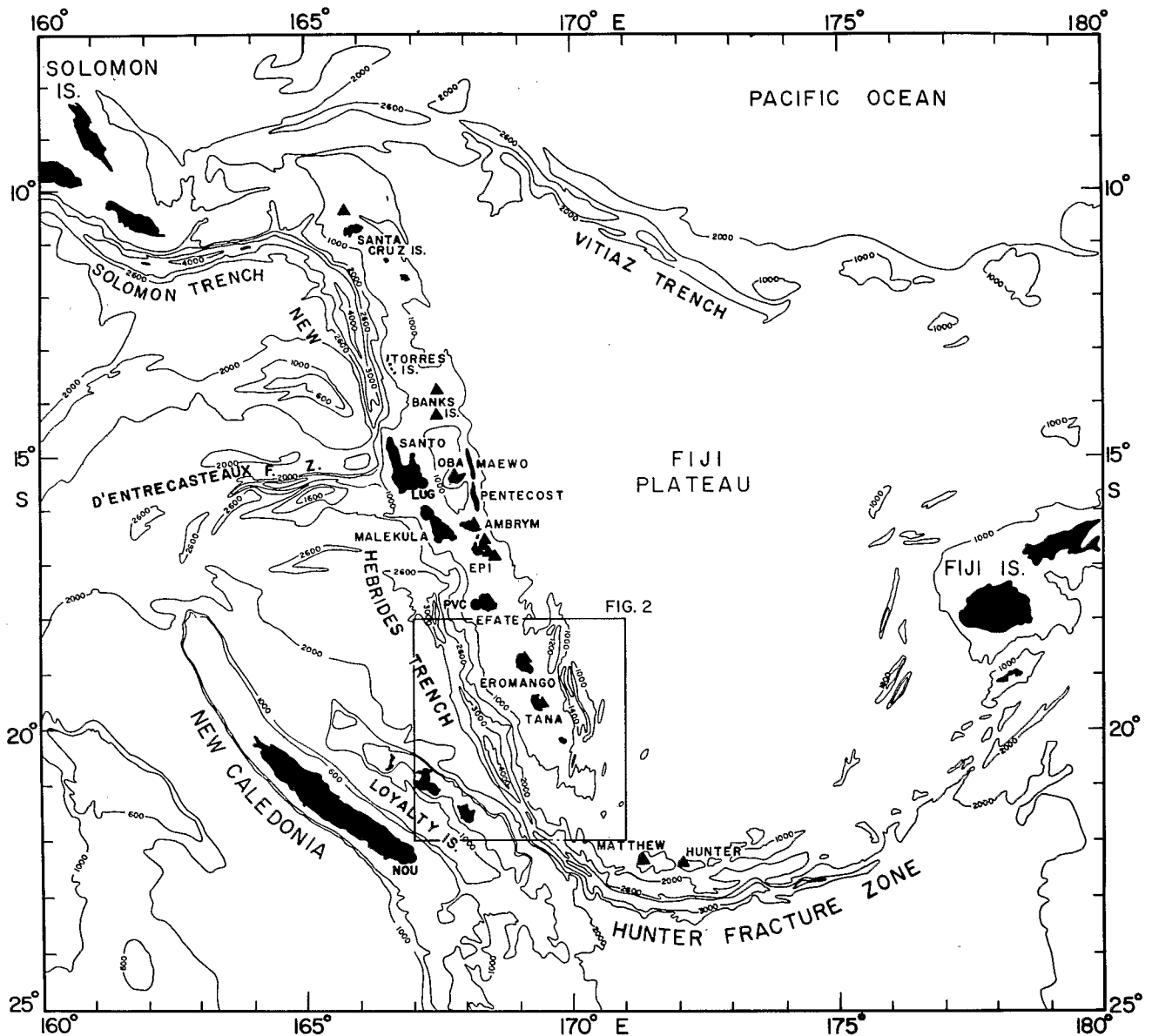
Fig. 1. Map view of the New Hebrides–Fiji area. The bathymetric contours are in fathoms [*Mammerickx et al.*, 1971].
The triangles indicate the active volcanoes. The central frame indicates the area studied in this paper.

results must take into account the limited time period sampled by the experiment. Several characteristics of the seismicity of the southern New Hebrides arc seem to be strikingly similar, however, both in the small-magnitude data recorded by the temporary network and in the data located by the worldwide network during the preceding 17 years.

In this study, homogeneous flat-layered velocity models were used for locations, even though the subduction zone almost certainly includes laterally heterogeneous structure. However, we concluded that locations within the network are sufficiently accurate to distinguish the major features on the scale of the network and of the section across the island arc. Comparisons of locations with different data sets and analysis of the travel time residuals obtained in the locations were examined carefully for effects of possible velocity anomalies associated with the structure of the arc, particularly those associated with the descending slab. The unusually wide coverage of both sides of the steeply descending slab would seem to provide a good opportunity to look for slab anomalies. The

surprising result of this study was that although anomalies were detected, they were rather subtle and appear to be attenuated by offsetting effects in the shallow structure of the arc.

Focal mechanism data were considered, including solutions for the large ($Ms > 6$) events for the preceding 17-year period and limited data from first motions recorded by the temporary network. In the latter case, clear results were difficult to obtain owing to limited coverage of the focal sphere and to serious uncertainties in the calculated positions of data on the focal sphere. For shallow events the basic problem was the determination of whether the first arrival is a direct or a refracted wave. Small changes in hypocentral depth or depth of an interface in the velocity model can cause large changes in the inferred positions of data on the focal sphere and thus have very serious effects on the focal mechanism solutions.

The operation of the temporary network was a cooperative project carried out by the French Office de la Recherche Scientifique et Technique Outre-Mer (ORSTOM), Cornell University, and the Marine Science Institute of the University of
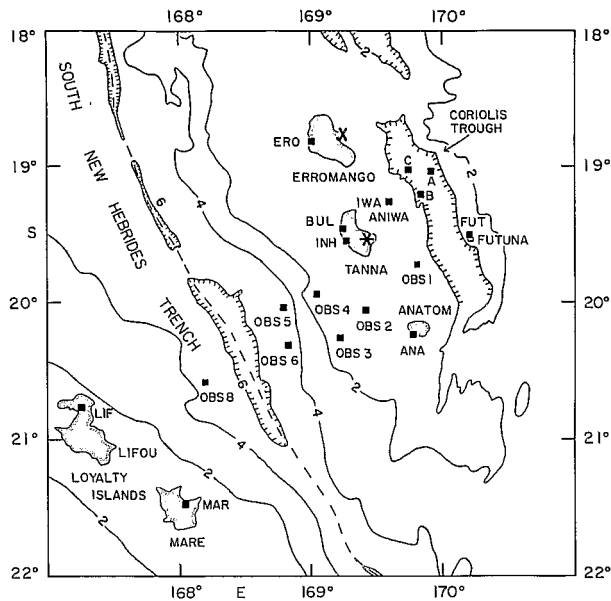
Fig. 2. Map of the southern New Hebrides arc. The squares indicate the locations of the stations of the temporary seismograph network (the land stations are denoted by three letter names, the OBS are numbered; A, B, C indicates the place of three OBS that operated for a 24-hour experiment). The bathymetric contours are in kilometers (from *Daniel* [1978] for 18°S to 20°S and interpolated from *Mammerickx et al.* [1971] for 20°S to 22°S). The cross indicates the location of the Quaternary volcano. The star shows the historically active volcano.

Texas. The ocean bottom seismographs were built by the University of Texas and are described by *Ibrahim and Latham* [1978]. *Ibrahim et al.* [1980] discussed results obtained from refraction profiling done as part of this cooperative project.

DESCRIPTION OF RECORDING NETWORK AND EARTHQUAKE LOCATION PROCEDURES

The locations of the seismic stations are given in Table 1 and shown in Figure 2. The coordinates of the ocean bottom seismographs (OBS) were obtained with the satellite positioning system of the N.O. *Coriolis* (CNEXO), the ship that re-

TABLE 1. Coordinates of the Seismic Stations of the 1977 Temporary Network

| Island	Name	Latitude, °S	Longitude, °E	Water Depth, m
Land Stations				
Erromango	ERO	18.82	169.01	
Aniwa	IWA	19.26	169.59	
Tanna	BUL	19.46	169.24	
Tanna	INH	19.55	169.27	
Futuna	FUT	19.52	170.20	
Anatom	ANA	20.24	169.77	
Lifou	LIF	20.77	167.24	
Mare	MAR	21.47	168.04	
OBS Stations				
OBS 1		19.73	169.81	1554
OBS 2		20.06	169.42	1408
OBS 3		20.26	169.22	558
OBS 4		19.94	169.05	1380
OBS 5		20.04	168.75	4770
OBS 6		20.32	168.82	4938
OBS 8		20.58	168.19	4282
OBS A		19.03	169.91	3000
OBS B		19.20	169.82	2800
OBS C		19.02	169.73	2600
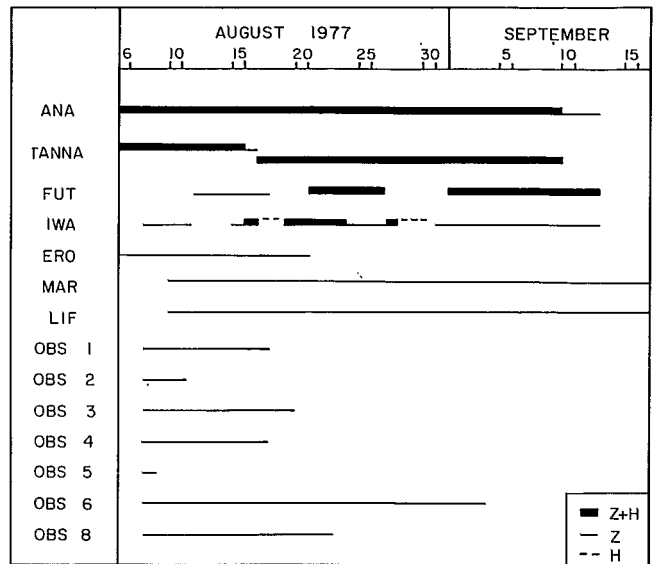
Fig. 3. Summary of the periods of operation of the local stations. Different symbols indicate the component of the ground motion recorded. Tanna includes INH and BUL; INH ran first, then the station was moved to the quieter site of BUL.

leased the seismographs. The eight OBS units recorded the analogue signals on magnetic tapes. Many of the OBS units suffered recording failures and operated only during the first part of the period, as shown in Figure 3. The land network included both analogue and digital recorders. Four Sprengnether MEQ-800 systems and two large recording-drum systems (modified versions of those described by *Ward et al.* [1969] recorded the signals on smoked paper. The land network also included six digital recorders (Sprengnether DR-100). All the stations had vertical component geophones, and some of the land stations had, in addition, a single horizontal component (Figure 3). All the seismometers for both land and OBS units were Mark Products geophones with a natural frequency of 4.5 Hz. Accurate GMT (WWVH) time corrections were available for the land stations throughout the recording period. The time correction of the OBS was interpolated from the GMT (WWVH) time before and after OBS immersion. The on-board OBS chronometers were highly stable and carefully rated under conditions equivalent to the ocean bottom.

From the numerous earthquakes recorded during the experiment, only those with at least three P arrival times and one S arrival time were located. About 250 earthquakes fulfilled this condition. P and S arrival times were weighted according to the record reader's judgement of the quality of the phase onset. The uncertainty in the determination of the arrival time of a good P or S phase was estimated to be less than 0.2 s and less than 0.5 s for S arrival times read on a vertical component record.

TABLE 2. Velocity Models Used in the Study

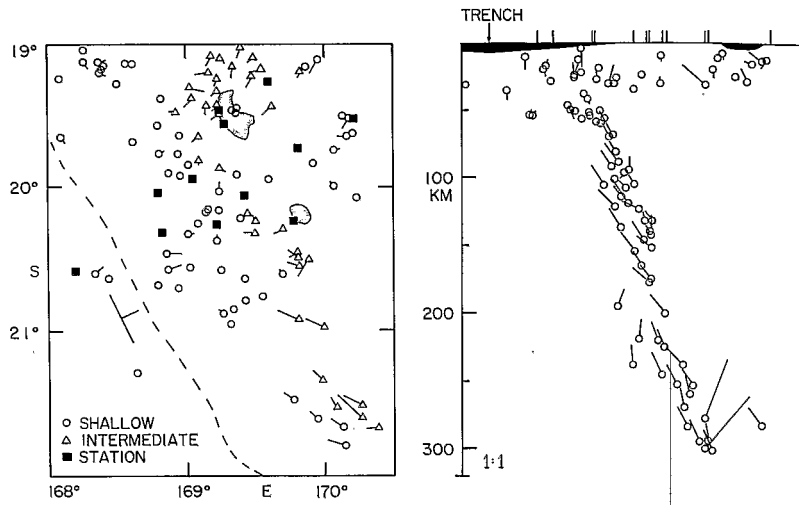| Model 1		Model 2	
Depth, km	Velocity, km/s	Depth, km	Velocity, km/s
00–15	5.55	00–12	5.2
15–33	6.44	12–30	7.2
33–150	7.77	30–100	8.06
150–	8.20	100–200	8.13
		200–240	8.17
		240–	8.20

Fig. 4. Variations of locations of earthquakes when two different velocity models are used. Included are class A to D locations. The symbols indicate the determinations obtained with the second model of Table 2, and the lines indicate the movement of these locations to the ones obtained with the first model of Table 2. On the map view (left) the dashed line indicates the location of the trench axis. Events north of 21°S have been reported on a vertical section (right). The trend of the projection is indicated by the two segments drawn on the map view near the trench axis. On the cross section (right), the vertical lines at the top of the section indicate the positions of the seismograph stations. Note the consistent pattern observed on the cross section for the intermediate-depth events. This indicates that the relative determinations of these events are little dependent on the velocity model (the discrepancy observed for several intermediate-depth events is restricted to quality C or D locations).

The locations were determined using the HYPO 71 computer program [Lee and Lahr, 1975]. Inputs to this program include a horizontally layered model for P wave velocities (Vp), a value for the ratio of P wave velocity to S wave velocity (Vp/Vs), and station corrections. Two velocity models were used (Table 2): one was a modification of the Jeffreys-Bullen (J-B) model, and the other was obtained from a compilation of the available information on the structure of the region [Dubois, 1969; Kaila and Krishna, 1978; Ibrahim et al., 1980]. The second model was an attempt to find a compromise between the different structures beneath the oceanic plate, the

arc-trench gap, and the arc itself. Although a clear choice between these two velocity models could not be made with the available data, the second model was chosen because it gave slightly better agreement between hypocenters determined by the local network and those determined by teleseismic data. However, the two models did provide a useful basis to explore the effects of model variations on the locations.

Many studies have shown the importance of shear wave data on the quality of the hypocentral determinations [James et al., 1969; Buland, 1976]. To use S arrival times, we estimated Vp/Vs from the slope of the function $Dt_s = (Vp/$
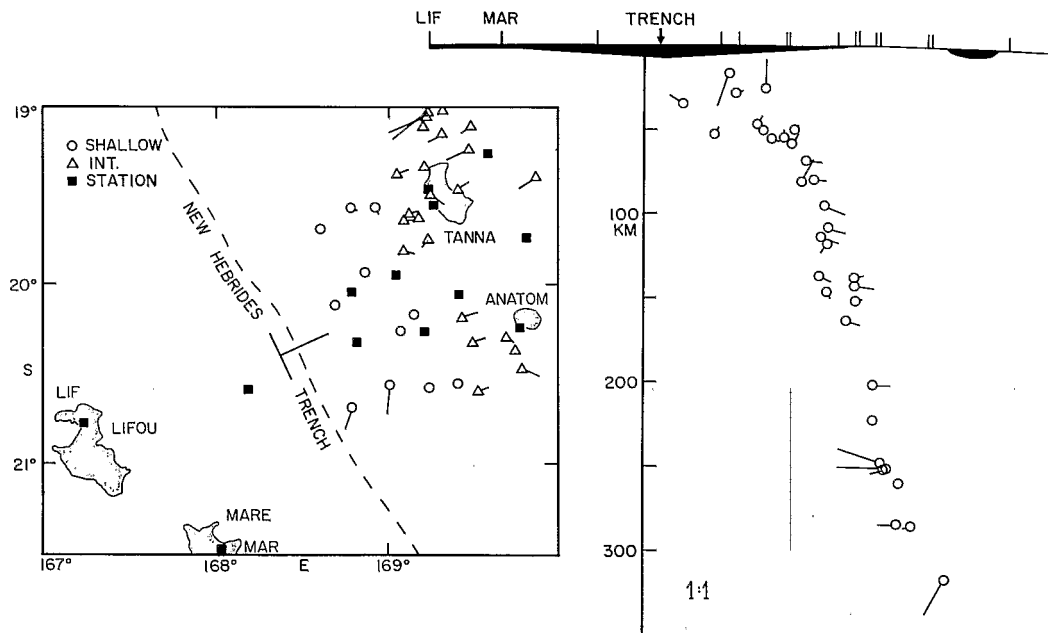

Fig. 5. Movement of the locations when data produced by Mare (MAR) and Lifou (LIF) stations are and are not used in the determinations. The symbols indicate the locations with all the data; the lines indicate the movement of the locations when MAR and LIF are excluded. The hypocenters shown on map view (left) have been reported on a vertical section (right); the location of the line of projection and its trend is indicated by the two perpendicular segments that cross the trench axis on the map view.

TABLE 3. Comparison of the Determinations of the Parameters of Four Events Located With Different Sets of Data

Date (1977)	Origin Time, UT	Latitude, °S	Longitude, °E	Depth, km	N	Source of Data
August 13	0959:41.4	19.27	169.18	144	53†	ISC and local
	0959:42.1	19.27	169.15	152	49	ISC
	0959:41.8	19.34	169.20	150	12	local (velocity model 2)
	0959:42.2	19.36	169.16	141	12	local (velocity model 1)
August 16	0615:17.9	19.29	167.73	20*	102†	ISC and local
	0615:18.3	19.26	167.67	20	102	ISC
	0615:18.5	19.28	167.67	31	17	local (velocity model 2)
	0615:17.8	19.28	167.68	25	17	local (velocity model 1)
August 25	0122:42.8	19.03	169.36	251	59†	ISC and local
	0122:48.5	19.02	169.32	256	52	ISC
	0122:48.6	19.16	169.32	250	8	local (velocity model 2)
	0122:49.8	19.25	169.31	237	8	local (velocity model 1)
August 26	1406:17.3	20.49	169.82	157	47†	ISC and local
	1406:17.5	20.53	169.82	159	42	ISC
	1406:17.7	20.56	169.79	156	12	local (velocity model 2)
	1406:18.1	20.53	169.69	150	12	local (velocity model 1)

N is the number of stations used (see Figure 6).
*Depth is fixed.
†This relocation was made with a J-B velocity model. Readings from stations reported by the ISC that have large residuals are not used in the combined ISC and local determinations.

$Vs)Dt_p$, where Dt_p and Dt_s are the arrival time differences of P and S, respectively, from the same earthquake at two stations. A least squares solution for 426 observations (all the earthquakes and all the station pairs) yielded $Vp/Vs=1.75$ with a 95% confidence level of 0.02. For comparison, the values of the J-B velocity model are 1.66, 1.74, and 1.78 for the upper crust, the lower crust, and the uppermost mantle, respectively. Attempts to differentiate Vp/Vs for shallow- and intermediate-depth earthquakes or for land and ocean stations did not give statistically significant differences [Coudert, 1980].

The station correction is an important factor in locating events by networks in which land and ocean bottom stations are used together. The structure beneath these stations is, in general, quite different. However, lacking sufficient information, we made a simple water depth correction for the OBS times. To the observed time, we added the time that a ray spends in a layer with a thickness equal to the water depth above the station and which has a velocity equal to the velocity of the first layer of the velocity model.

The accuracy of a location is also a function of the quality of the arrival time data, the network geometry, and the position of the hypocenter relative to the network [Peter and Crosson, 1972; Lilwall and Francis, 1978; Chatelain et al., 1980]. The quality of the locations of the earthquakes were carefully graded according to these parameters. Four grades were assigned. Grade A determinations were the best and were based on all of the following criteria: (1) The locations of the earthquakes were determined with abundant P and S data, (2) the recording network had a good configuration, i.e., it had a sufficent aperture that was relatively constant with respect to azimuth, (3) the depth of the hypocenter was comparable to the spacing between stations in the network, (4) the epicentral distance to the nearest station was less than the depth of the earthquake, and (5) the mean residual and the residual at the nearest station were reasonable. Grade B determinations were also considered good, but not all the conditions required for grade A were fulfilled. Grade C was assigned to shallow earthquakes with reasonably well-located epicenters but with no near observations to constrain the depth accurately or was assigned to intermediate-depth earthquakes with constraint on the depth but with less constraint

on the epicenter because of the small aperture of the locating network relative to the depth. Grade D was assigned to the determinations that were less reliable, such as those with insufficient data or with a bad configuration of the recording network.

Tests were performed to study the dependence of the locations on the velocity model, the ratio of Vp/Vs, and station corrections [Coudert, 1980]. Hypocenter determinations were compared when one of these values was changed. Figure 4
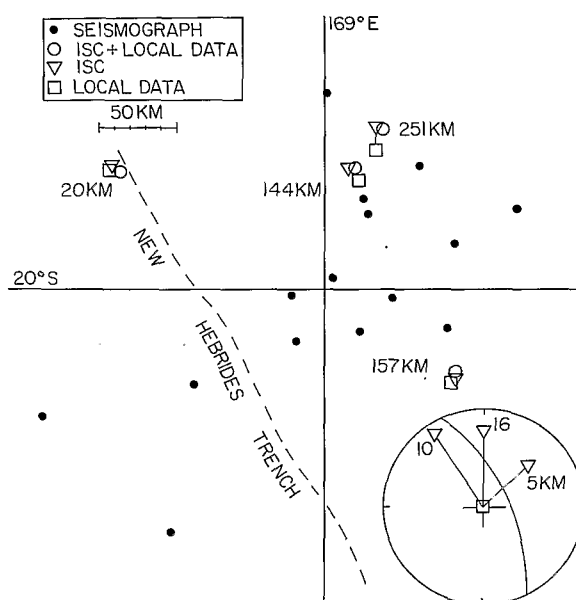

Fig. 6. Comparison of the determinations of the four events located by both the ISC and the local network. The symbols indicate locations obtained with different sets of data (see Table 3): The squares indicate locations obtained with the local data and the fast velocity model. On the bottom right, the difference between local and ISC hypocenter determinations of the three intermediate events are plotted on an equal area projection; the radius is normalized to the value of the difference (10, 16, and 5 km for the events at a depth of 144, 251, and 157 km, respectively). This plot gives a three-dimensional view of the difference and shows that the locations have a good depth fit. The strike of the descending plate is also shown on the focal sphere.
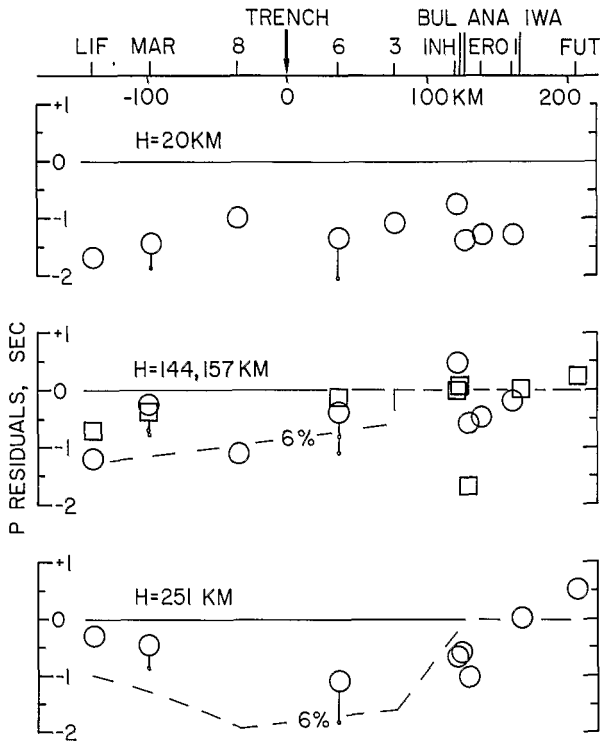
Fig. 7.   P wave residuals observed at the local stations when the location is made with both local and worldwide P data plotted versus the distance from the stations to the trench axis. The dashed lines indicate the residual obtained for a two-dimensional model with a 70-km-thick slab dipping 70° with a 6% high-velocity anomaly at depths larger than 70 km. The symbols on Mare and OBS 6 data show the observed residuals; the dots show the corrected residuals. The corrections deduced from the study of residuals from the local events (Figure 8) are +0.4 and +0.7 s, respectively. The circles and squares for the center figure are for the earthquakes at 144 and 157 km, respectively.
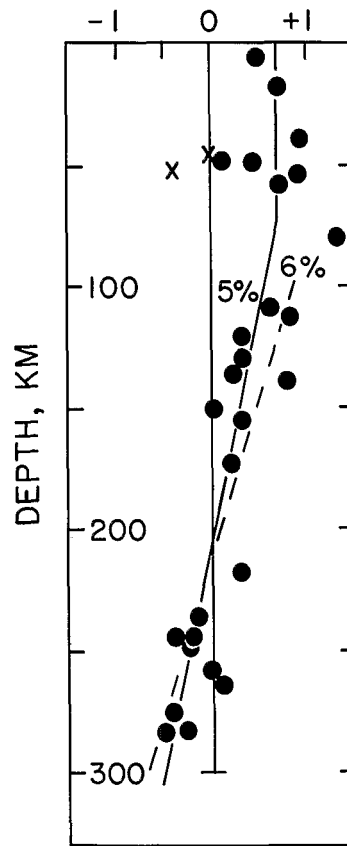

Fig. 9.   Interpretation of P residuals observed at OBS 6. The least squares fit of the data at depths larger than 100 km with a straight line corresponds to a 5% high-velocity anomaly associated with the medium crossed by the ray paths to OBS 6. The pattern produced by a 6% high-velocity anomaly is also shown (dashed line).

shows, for example, the variation of the determinations when two different velocity models were used. This test provided a way to check the quality of the determinations, and a poor quality, grade D, was assigned to the shallow epicenter determinations that varied too much (more than 10 km) when the two different velocity models were used. From such tests it was observed that when the determination was performed with enough data and the epicenters were in or near the network, the absolute positions of the hypocenters of shallow

earthquakes and the relative positions of the intermediate-depth earthquakes were little dependent on a reasonable variation in the velocity model, Vp/Vs, or a station correction change.

A more important effect on the precision of the relative positions of the hypocenters was the variation in the effective configuration of the recording network during the experiment.
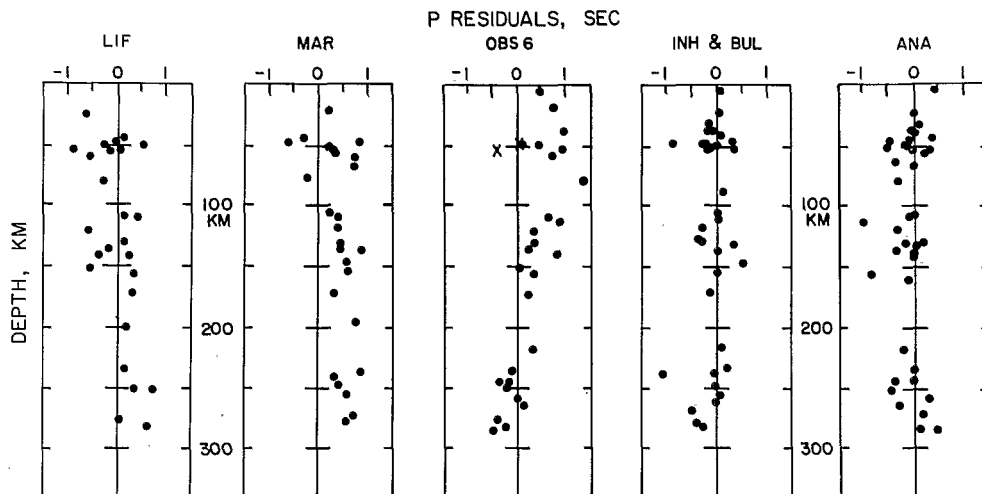

Fig. 8.   P wave residuals as a function of hypocentral depth for several local stations. Only A and B quality locations obtained with the second velocity model of Table 2 and determined with at least nine arrival times are included. Tanna data include readings for BUL and INH.
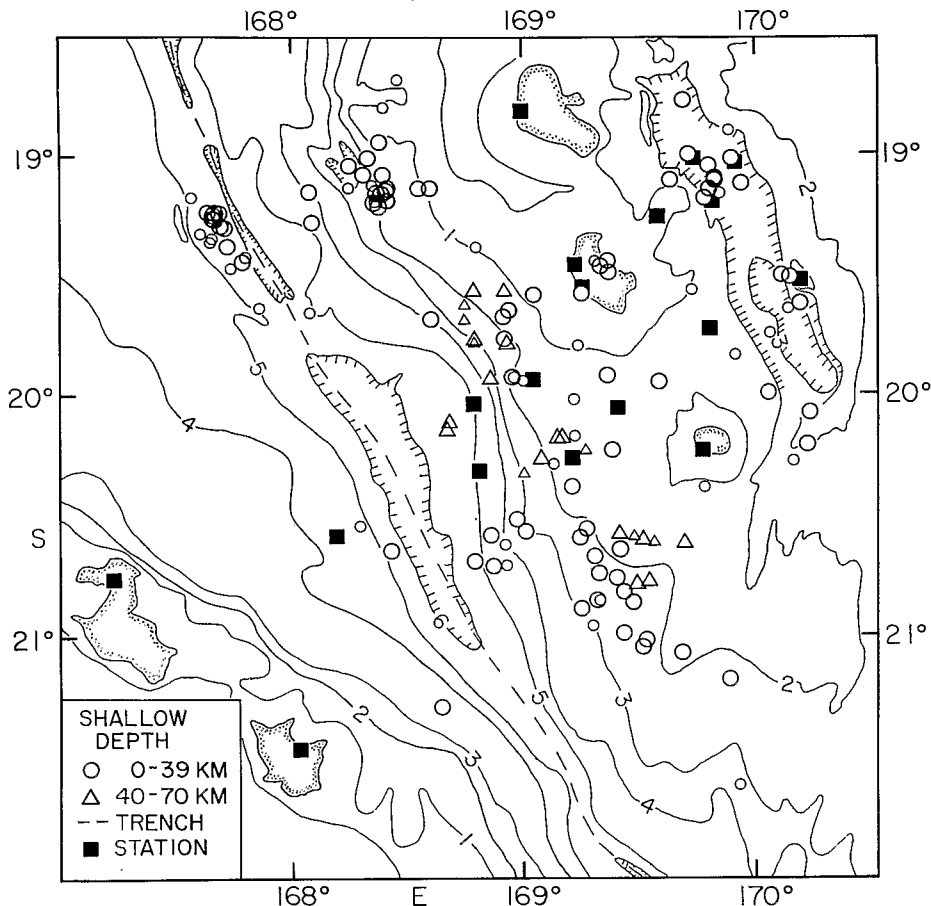
Fig. 10. Map showing epicenters of shallow earthquakes determined by the local network. The large symbols represent A, B, and C quality locations, and the small symbols represent the D quality epicenters. Solid squares represent the seismic stations of the temporary local network. The bathymetric contours are in kilometers.

Since the recording time of the OBS was short, and the later locations were made with mostly the land station data, several tests were made on events that occurred early in the experiment and were recorded by both land and many of the OBS stations. No systematic variations were observed in the locations determined successively with the OBS stations alone, the land stations alone, and then with the OBS and the land stations. The observed differences were mostly less than 10 km. The Mare (MAR) and Lifou (LIF) stations (see Figure 2) were installed on August 10 and were not included in the determinations of events recorded during the first few days of the experiment. Moreover, since they were distant from the active region, they did not record the small-magnitude events. Figure 5 shows that when the data of these stations are used, the determinations are systematically different (as discussed in the next section) from the determinations obtained when these data are not used. These differences are mostly less than 10 km except when few data are used.

From all the above studies the relative precision of the determinations was estimated to be about 10 km for most of the 'B' quality events. Some events had a better precision (A quality) but were not numerous enough to be considered alone. The 'C' quality locations included shallow earthquakes that had epicenters determined well to within 10 km but with an uncertainty of depth between zero and about 50 km. The 'C' quality intermediate earthquakes had depths known to within 10 km, but the epicenter was known only to within a few tens of kilometers.

All these considerations ignore the effects of laterally heterogeneous structure. In the next section, evidence is sought for such structure in terms of mislocations and travel time residuals derived from the computations with flat-layered models.

EFFECTS OF LATERAL HETEROGENEITIES ON EARTHQUAKE LOCATIONS

Comparison of Locations Based on Local and on Teleseismic Data

Because of the lateral heterogeneities associated with subducting plates a bias on the location of the earthquakes can be induced with worldwide data as well as with data from local networks [see, e.g., *Mitronovas and Isacks*, 1971; *Utsu*, 1975; *Engdahl et al.*, 1977; *Hasegawa et al.*, 1978; *Barazangi and Isacks*, 1979]. Some of these authors note that, in general, the local determinations of hypocenters tend to show the Benioff zone steeper than it is and that this bias is reduced when a high-velocity zone associated with the subducting slab is taken into account.

During the New Hebrides experiment, several earthquakes recorded by the local network were large enough also to be located by the International Seismological Centre (ISC). These locations determined from teleseismic data can be compared with those from local data (see Table 3). In addition to the local and ISC determinations, locations were obtained using P arrival times reported by the ISC plus all the local P readings. For these relocations, the J-B travel time tables were used.

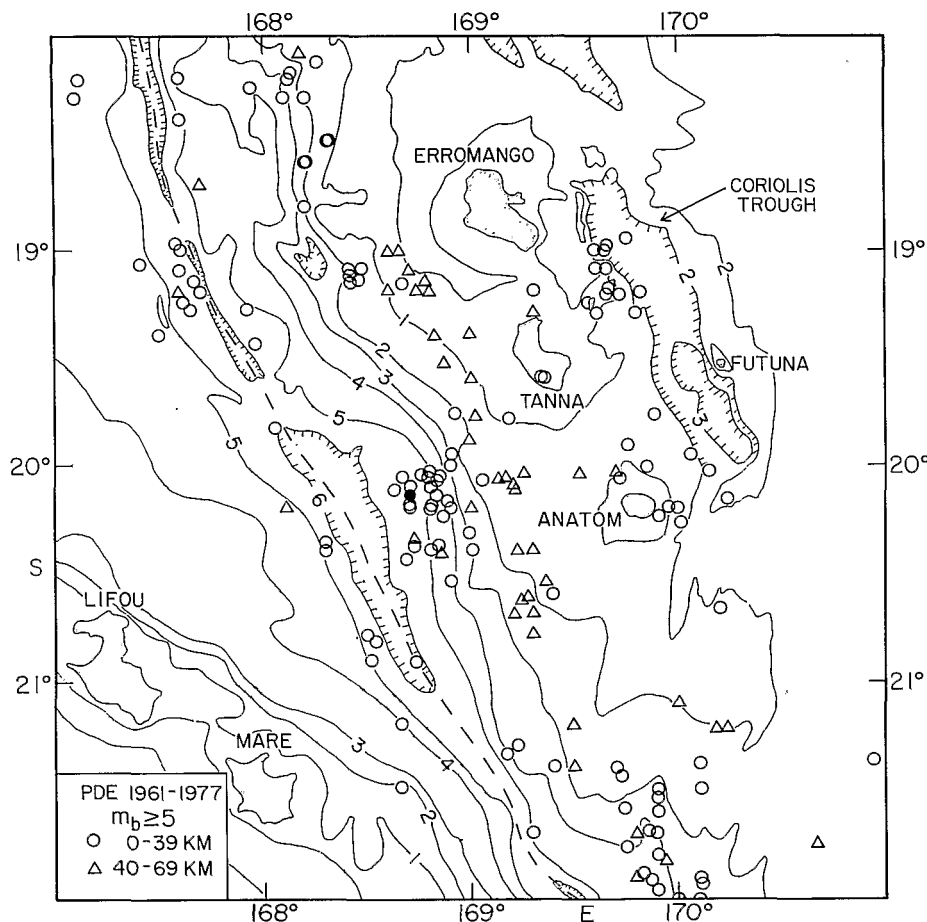For a shallow earthquake ($Ms = 4.9$) located beneath the

Fig. 11.   Map showing locations of the shallow events of $Mb \geq 5$ reported in the PDE for 1961–1977. Bathymetric contours are in kilometers. The solid circle indicates the location of the $Ms = 6$ event that occurred in the region in 1978.

trench axis, epicenters determined by the ISC, the local P and S readings, and the combined teleseismic and local P readings are all within 7 km of one another (see Figure 6). This is quite remarkable in view of the large lateral changes in structure that must exist in this active island arc. It is possible that the use of data from some of the permanent local stations of the French ORSTOM network in the New Hebrides–New Caledonia region for the ISC locations partly accounts for the smallness of the observed changes.

For the three intermediate-depth events (Table 3) the locations determined with the local P and S data, and the faster of the two velocity models (see Table 2) is in best agreement with the ISC locations. With the fast model the hypocenters differ only by distances of 10, 5, and 16 km, for the events at depths of 152, 159, and 256 km (Figure 6), respectively. The locations determined with both local and teleseismic P data differ by less than 5 km from the ISC locations and have slightly shallower depths. However, as the dip of the Benioff zone is steep in the New Hebrides, these small differences can produce variations in the dip of this zone. When located with local data, two of the three intermediate-depth events in Figure 6 show a steeper Benioff zone than that obtained from teleseismic data. This is also suggested in Figure 18, in which the seismicity obtained from local data is compared with the Benioff zone obtained from a 14-year sample of good ISC locations. At depths larger than 200 km the local data tend to show the Benioff zone to be slightly steeper than do the worldwide data. This result is similar to, but not as large as, that reported in other areas.

Lateral Heterogeneities in the Crust and Upper Mantle.

Two different kinds of lateral heterogeneities are expected in the region covered by the network. First, there are variations in the crustal structure along a cross section perpendicular to the trench [e.g., *Collot and Missegue*, 1977; *Ibrahim et al.*, 1980]. Second, high-velocity anomalies of 5 to 11% are usually associated with the descending plates in the upper mantle.

No clear effect of the first kind of heterogeneity could be obtained in the present study. Figure 7 shows the residuals (observed minus computed travel times) for P arrivals at the local stations for the four events whose locations were determined with both local and worldwide data (see Table 3). These residuals are a combination of the effects of velocity anomalies and the mislocation of hypocenters. For the shallow event the maximum difference of 1 s between the observed residuals may be due to the first kind of heterogeneity (i.e., crustal). However, no simple pattern appears. For example, there is no clear difference between the residuals at stations located to the east and to the west of the trench.

Several indications of the second kind of heterogeneity were obtained. On Figure 7, the dashed line shows the anomaly produced by a model in which a 6% high-velocity zone is located at depths larger than 70 km and is associated with a 70-km-thick slab that has a 70° dip. The data for the three intermediate-depth events show some slight agreement with the predicted trends, but the noise level is rather high. Study of the local data alone gives further indication of a possible ef-
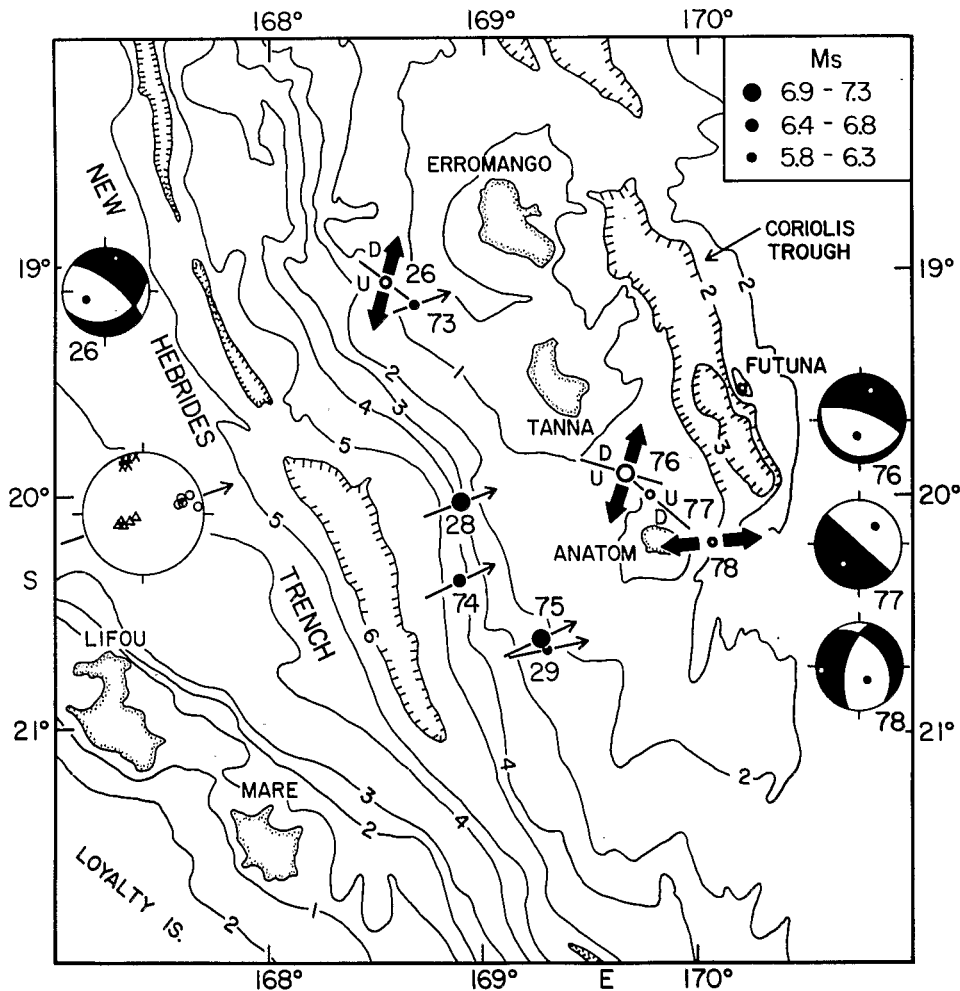
Fig. 12. Map showing focal mechanisms of shallow activity in southern New Hebrides. This figure includes all the published focal mechanisms and new solutions for the period 1963–1976. The events are numbered as in Table 4. The bathymetric contours are in kilometers. The size of the circles indicates the magnitude of the events. Slip vectors for solutions showing underthrusting (solid circles) are indicated by arrows. The poles of the nodal planes and the null axes (crosses) of these five events are reported on a lower hemisphere stereographic projection on the left side of the figure. The intraplate focal mechanism solutions are shown on stereographic projections of the lower hemisphere; the solid quadrants are compressional first arrivals. The epicenters (open circles), the strike of the high angle nodal planes, and the interpretation of the main stress are shown in map view.

fect of the descending slab. Figure 5 shows the variation of the determinations when the Loyalty stations (MAR and LIF) are excluded or used in the locations. For events between depths of about 70 and 200 km, the Loyalty Islands data tend to pull the earthquake determinations toward the west, an effect that could be explained by a high-velocity zone associated with the subducting slab. At depths larger than about 250 km the observed reversal of the bias in the locations could be the result of ray paths traversing the lower-velocity, upper mantle material that exists beneath the descending plate on their way to the Loyalty Islands stations. An alternative explanation for the above reversal in the bias is that excluding the Loyalty stations from the locations makes the network aperture narrower. This particularly affects the deeper events and results in a relatively steeper inclined seismic zone. This explanation is in accordance with the results reported by *Hasegawa et al.* [1978] for the Japanese arc.

Further indication of the high-velocity zone was found in the pattern of the residuals for the *P* arrival times of events located only by the local network. Although the pattern of residuals will be affected and perhaps confused by the variations

in stations used for locations and by the least squares minimization of residuals by the location procedure, we can still find interesting patterns for several of the stations. Figure 8 shows the *P* residuals as a function of the depth of the earthquakes. For the land stations located near the volcanic arc (ANA, BUL, and INH) the residuals have a nearly zero mean and a standard deviation less than 0.3 s. Residuals for MAR are positive throughout the range of depths by about 0.4 s. This can be interpreted as a station effect. The standard deviations at LIF and OBS 6 are larger than the preceding ones. The location of OBS 6 and the clear variation of residual with depth suggest the effect of a high-velocity descending slab. The least squares fit of the decrease in the residual pattern with respect to depth for events between depths of 80 and 300 km gives a variation of 0.006 s/km with a 95% confidence interval of 0.001 s/km. For a medium with a velocity of 8.0 km/s, this corresponds to a high-velocity anomaly of 5% (± 1%) (Figure 9). Since the OBS 6 data were used in the locations, the residuals tend to be minimized; therefore this 5% value is a lower limit for the real velocity anomaly.

The other remarkable feature of the OBS 6 residuals is that

TABLE 4. Parameters (as Reported by the ISC) of Earthquakes With Determined Focal Mechanisms

Event	Date	Latitude, °S	Longitude, °E	Depth,* km	References
		Shallow Events			
26	March 9, 1970	19.07	168.54	19†	*Pascal et al.* [1978]
28	Nov. 2, 1972	20.03	168.91	27†	*Pascal et al.* [1978]
29	Dec. 7, 1968	20.62	169.32	68	*Johnson and Molnar* [1972]
73	Feb. 24, 1973	19.16	168.68	36†	this study
74	Sept. 13, 1972	20.33	168.79	21†	this study
75	Aug. 2, 1976	20.59	169.31	43	this study
76	Dec. 9, 1973	19.90	169.67	26	this study
77	March 3, 1974	20.01	169.77	14†	this study
78	July 28, 1976	20.20	170.07	5	this study
		Intermediate Events			
51	April 20, 1970	18.79	169.29	248	*Pascal et al.* [1978]
52	May 1, 1963	19.09	169.04	134	*Isacks and Molnar* [1971]
53	March 30, 1963	19.11	169.01	166	*Isacks and Molnar* [1971]
54	Dec. 21, 1966	19.96	169.74	228	*Isacks and Molnar* [1971]
55	Jan. 20, 1964	20.70	169.92	139	*Isacks and Molnar* [1971]
56	Oct. 7, 1966	21.59	170.56	162	*Isacks and Molnar* [1971]
79	July 23, 1974	19.55	169.37	140	this study
80	Jan. 28, 1972	19.38	169.13	117	this study
81	Oct. 13, 1969	18.78	169.31	251	this study
82	March 17, 1973	19.41	169.39	187	this study
83	March 13, 1975	21.75	170.53	72	this study

*The depths obtained by ISC from pP observations have been reported for intermediate depth events when available.

†Depth obtained from synthetic waveform of long-period P waves (after D. Chinn and B. L. Isacks, manuscript in preparation, 1981).

they are positive for depths less than 200 km. The effect of the high-velocity slab, seen in the decrease in residuals with depth, is offset by a low-velocity anomaly located at shallow depths. The source of the positive anomaly, however, is difficult to resolve. All the shallow-depth events that show clear positive residuals are located near the inferred zone of contact of the two plates (circles in Figure 9). At 50-km depth, of the three earthquakes without significant positive residuals at OBS 6, two are inside the subducting plate (crosses in Figure 9). Moreover, the residuals at OBS 6 from the large shallow earthquake (mainshock of August 16, see Table 3) and its aftershocks, which occurred northwest of the network beneath the trench, are near zero (for six events the average residual is +0.2 s with a 0.2-s standard deviation). This observation is confirmed by the relative residual of the main event when the determination is performed with both local and worldwide data (see Figure 7). The residual is close to that for all the local stations and is not relatively positive. These data thus do not support a simple station correction to account for the observed positive residuals at OBS 6 for events on the arc side of the trench. All the events near the thrust zone are east of the OBS 6 station; therefore it is possible that the positive residuals for these events are due to a mislocation of the station. However, the magnitude of the station mislocation implied is improbably large. The simplest interpretation involves a low-velocity zone along the ray paths from events located in the thrust zone and at intermediate depth such that the entire curve of residuals versus depth has a positive offset. This anomaly may be related to a property of the inclined zone of thrust faulting [*Louat et al.*, 1979] and/or to a low-velocity anomaly associated with the subducted oceanic crust. The observation of relatively low residuals at stations near the trench was also suggested in the data of *Mitronovas and Isacks* [1971] for the Tonga arc and was clearly observed in Japan [*Suyehiro and Sacks*, 1979].

In summary, although the data show evidence for a high-

velocity descending slab, the effects are subtle and do not induce a large bias in the locations. We think that the particular features of the New Hebrides arc can explain this paradox. The steep dip of the Benioff zone allows a sampling of the width of the arc without deploying a large network. Also, for a given depth, the length of the rays from intermediate-depth earthquakes is shorter in a steeply dipping slab than in a more gently dipping slab. The opportunity to have stations on both sides of the arc considerably reduces the amplitude of bias. The occurrence of a positive anomaly at shallow depth in the ray paths to the station near the trench also tends to balance the slab effect.

SPATIAL DISTRIBUTION AND MECHANISMS OF SHALLOW EARTHQUAKES

The shallow events located by the network are shown on Figure 10. The distribution of the events is quite uneven. Two clusters located north of the network correspond to aftershocks of two earthquakes with magnitudes (Ms) near 5.5 and 4.9, one located in the arc-trench zone and the other located seaward of the trench axis within the suboceanic plate. A gap in shallow activity is located to the south of the first cluster in the arc-trench region. Otherwise, epicenters are scattered beneath the arc-trench zone, with some concentration south of Anatom, and a few events are located beneath and seaward of the trench. In the back arc area, seismicity is located near and beneath the Coriolis trough.

Figure 11 shows the epicenters of moderate size events reported in the preliminary determinations of epicenters (PDE) for the period 1961–1977. The selection sought events with magnitudes (mb) larger than 5 (J.-M. Marthelot et al., manuscript in preparation, 1981). Figure 12 presents the published focal mechanisms [*Johnson and Molnar*, 1972; *Pascal et al.*, 1978] and new solutions (Tables 4 and 5) of all shallow events for the period 1963–1976 large enough ($Ms > 5.7 - 6$) to provide sufficient long-period data for a focal mechanism solu-

TABLE 5. Parameters of New Focal Mechanisms Determined in This Study

Event	Date	Origin Time, UT	Locations Latitude, °S	Locations Longitude, °E	Depth, km	Pole 1 Trend	Pole 1 Plunge	Pole 2 Trend	Pole 2 Plunge	P Axis Trend	P Axis Plunge	T Axis Trend	T Axis Plunge
73	Feb. 24, 1973	0738	19.16	168.68	36*	70	40	250	50	250	05	70	85
74	Sept. 13, 1972	1433	20.33	168.79	21*	65	20	245	70	245	25	65	65
75	Aug. 2, 1976	1055	20.59	169.31	43	65	34	245	56	245	11	65	79
76	Dec. 9, 1973	1955	19.90	169.67	26	17	74	197	16	197	61	17	29
77	March 3, 1974	1422	20.01	169.77	14*	40	00	...	90	40	45	220	45
78	July 28, 1976	1715	20.20	170.07	5	105	28	234	50	152	61	264	12
79	July 23, 1974	1058	19.55	169.37	140	110	20	218	40	258	12	156	44
80	Jan. 28, 1972	0116	19.38	169.13	117	144	66	324	24	324	69	144	21
81	Oct. 13, 1969	0656	18.78	169.31	251	90	20	270	70	270	25	90	65
82	March 17, 1973	0457	19.41	169.39	187	52	06	232	84	232	39	52	51
83	March 13, 1975	1845	21.75	170.53	72	120	10	300	80	120	55	300	35

Event numbers are a continuation of the numbering system of Pascal et al. [1978] and Isacks et al. [1981]. Locations are from the Bulletins of the ISO. Trend is measured clockwise from north; plunge is measured from the horizontal.

*Obtained from synthetic waveform of long-period P waves (after D. Chinn and B. L. Isacks, manuscript in preparation, 1981).

tion. For some of these earthquakes, D. Chinn and B. Isacks (manuscript in preparation, 1981) estimate the source depth from comparison of observed and synthetic P wave forms. The combination of these data sets yields new information on the shallow activity in this part of the New Hebrides island arc.

The Thrust Zone Between the Descending and Overriding Plates

Most of the large-magnitude events that occurred beneath the trench-arc region have thrust-type focal mechanisms (Figure 12, events 73, 28, 74, 75, and 29) interpreted as occurring at the boundary between the descending and overriding plates. The focal mechanism solutions indicate a direction of convergence of the oceanic plate with respect to the island arc of 070° (±5°), which is the same direction as that found in the northern part of the arc [Pascal et al., 1978]. The surprising result from data produced by the temporary network is the very low activity located along or near the assumed interface boundary in the central and northern parts of the network. If we exclude the aftershock activity associated with the July 10 event ($Ms = 5.5$) located in the arc-trench gap to the north of the network, little seismic activity seems to be located along the thrust zone north of Anatom (Figure 13, section north). South of Anatom, the activity increases (Figures 10 and 13) and may be related to the thrust zone, although depths are not well-constrained.

This distribution of the activity near the thrust zone seems to be correlated with the spatial distribution of the activity of larger magnitude events. The cluster of activity seen in the PDE locations (Figure 11) beneath the 4-km isobath at about 20°S includes aftershocks of the large ($Ms = 7.0$) event of 1972 (event 28, Figure 12). This region was very quiet during the operation of the temporary network in 1977. In 1978 an earthquake with a magnitude (Ms) of 6 occurred in the quiet area (solid circle in Figure 11). The gap of shallow activity located in the center of the network may be a precursory phenomenon for the 1978 earthquake. However, we cannot rule out the possibility that this gap is an effect of the short recording time. The relatively high activity located in the 1977 experiment southwest of Anatom under the 2-km isobath (Figure 10) is near the August 2, 1976, earthquake ($Ms = 6.9$, event 75; Figure 12) and may represent long-term aftershocks of that event. These observations, combined with those made during other short-term experiments in the central New Hebrides [Isacks et al., 1981], suggest that the small-magnitude background activity does not define the plate boundary very well except in the case of aftershocks of large earthquakes. A similar result is also reported for the Aleutian convergent plate boundary by Davies and House [1979].

The locations of the large events for which focal mechanisms and reliable depths were determined are shown in Figure 13. The dips of the nodal planes inferred to be the fault planes for the three thrust events (event 73 for section 'north,' events 28 and 74 for section 'south') are also indicated. The locations and dips of the inferred slip planes of the large events, as well as the distribution of small events, provide an estimate of the location and geometry of the plate boundary, as indicated in Figure 13.

Figure 14 shows the number of events, along with the cumulative number of events, recorded at Tanna, Anatom, and OBS 6 stations plotted as a function of (S-P) times. At Tanna a change in the rate of the cumulative number of events occurs at 6-s (S-P) time. This corresponds to the shortest distance between the inferred boundary of the interplate thrust
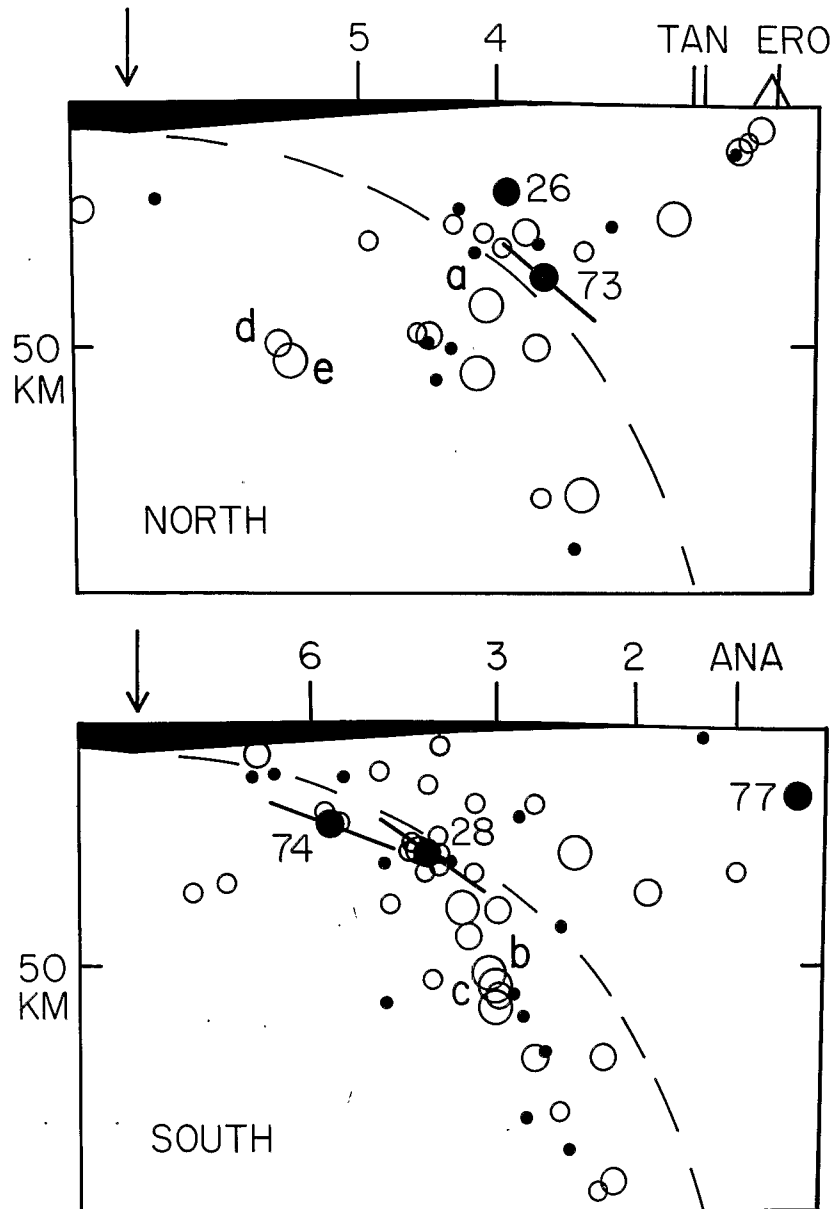
Fig. 13. Cross sections showing the shallow activity near the thrust zone. The limits of the sections are shown on Figure 16. This is an enlargement of part of Figure 17 (see Figure 17 caption for symbols explanation). The large solid circles represent the position of the large events whose depths have been estimated from synthetic seismograms. The line that crosses these symbols indicates the direction of the fault plane of the thrust events obtained from focal mechanism study (see Figure 12). These events are numbered following Table 4. For clarity, we have not reported on the section the two swarms of shallow activity located near 19°S on Figure 10. The letters indicate the local events that have focal mechanism solutions (see Figure 15). The heavy dashed line is an interpretation of the location of the plate boundary. It is the same line for both north and south sections.

zone and Tanna and suggests that this increase in the rate is probably related to the activity along the thrust zone. However, at Anatom the observed change in the rate of the cumulative number of events occurs at 5-s (S-P) time, while the shortest distance between Anatom and the interplate thrust boundary corresponds to about 6.5-s (S-P) time. This could be interpreted as an indication of a small change (about 10 km) in the geometry of the thrust zone near Anatom. This interpretation is not favored, mainly because of all the events with (S-P) times between 4 and 7 at Anatom that are located by the local network, the majority occur in the upper plate near the Coriolis trough. Hence the observed increase in the rate of cumulative number of events at 5-s (S-P) time probably corresponds to a back arc activity in the upper plate.

The OBS 6 histogram suggests a relatively low level of activity along the interplate boundary immediately below the station. This is in agreement with the results shown in Figure 13, which indicates an increase in seismic activity located farther east and toward the island arc relative to OBS 6. The relatively low level of activity near the shallowest part of the interplate boundary near the trench is also found in other parts of the New Hebrides [Isacks et al., 1981] and in other areas [e.g., Davies and House, 1979].

Shallow Seismic Activity Within the Descending Plate

Many shallow events determined by the local network (Figure 13) appear to be clearly located beneath the plate boundary and within the subducting plate. This observation is in
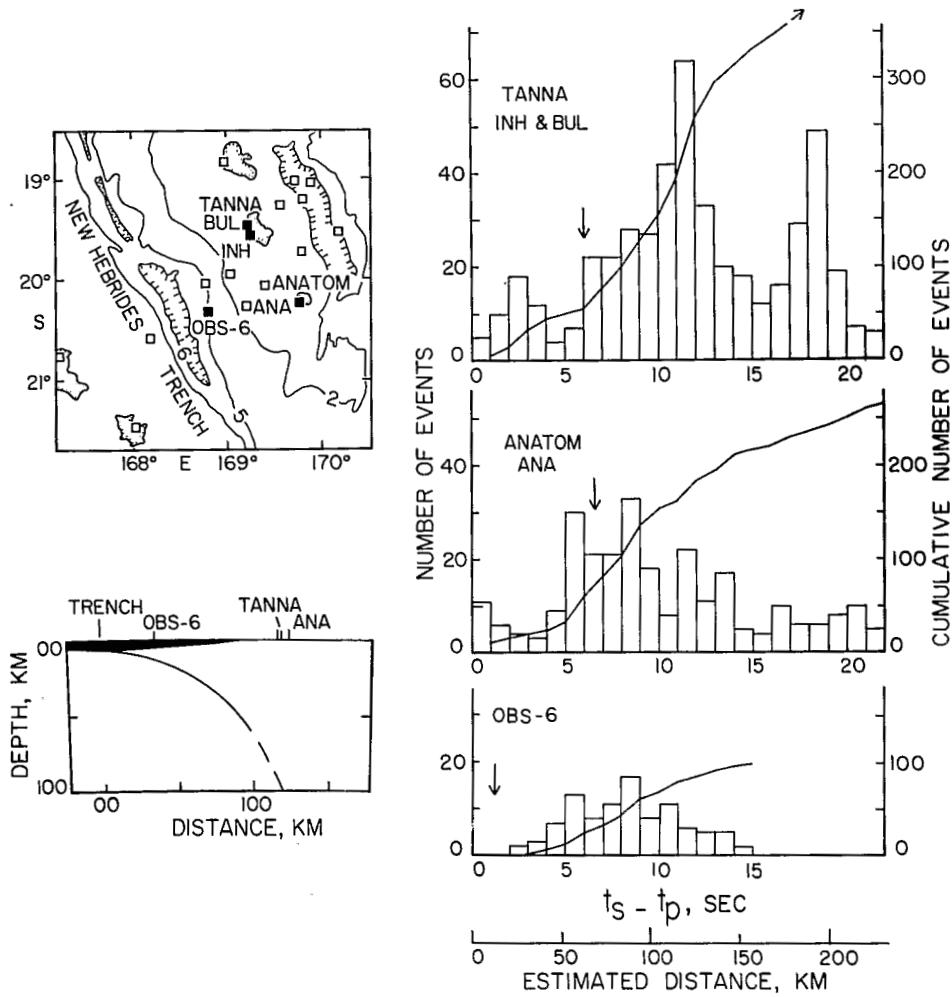
Fig. 14. The graphs on the right show histograms of the number of events, as well as the cumulative number of events, versus the difference between S and P travel times for three seismic stations of the local network. The locations of the stations are shown as solid squares on the map view. The arrows on the histogram plots correspond to the shortest distance between the three stations and the inferred boundary (from Figure 13) of the interplate thrust zone (as shown in the section in the lower left side of the figure).

agreement with the interpretation of limited first-motion data produced by the local network. Near the plate boundary, three events (a, b, and c, Figure 13) with enough first-motion data to allow a discrimination between thrust or normal fault-ing focal mechanisms were studied. None can be interpreted as thrust mechanisms (see Figure 15). These earthquakes have depths between 40 and 55 km. The nature of the mechanisms indicates that the microseismicity inside the subducting plate
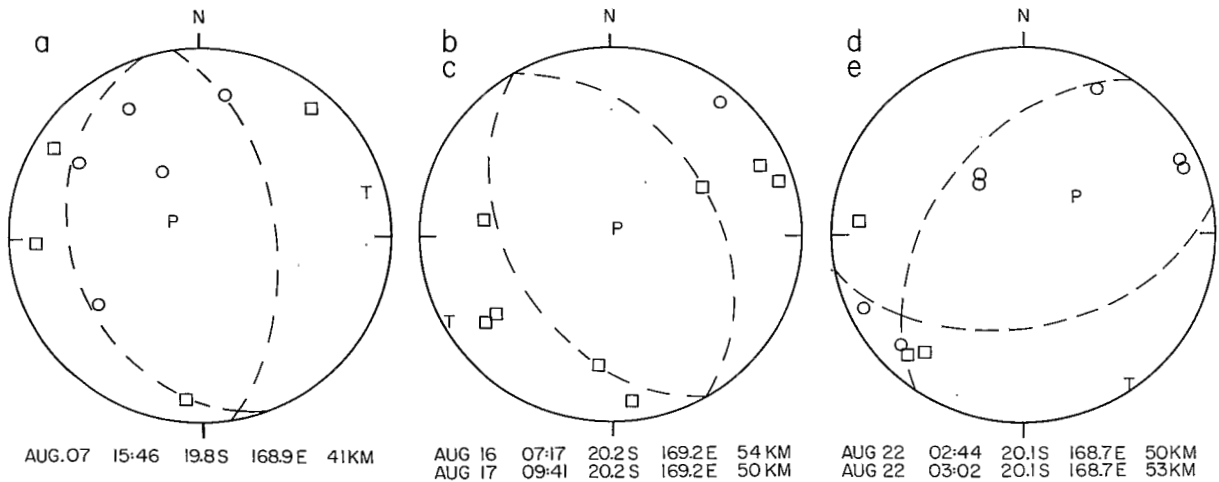

Fig. 15. First motions recorded at the local stations plotted on equal area projections of the lower hemisphere of the focal spheres. The squares indicate compressional first motions, and the circles indicate dilatational first motions. The dashed lines show an interpretation of the focal mechanisms. The parameters of the events are indicated under the focal sphere. The events are lettered as shown on Figure 13.
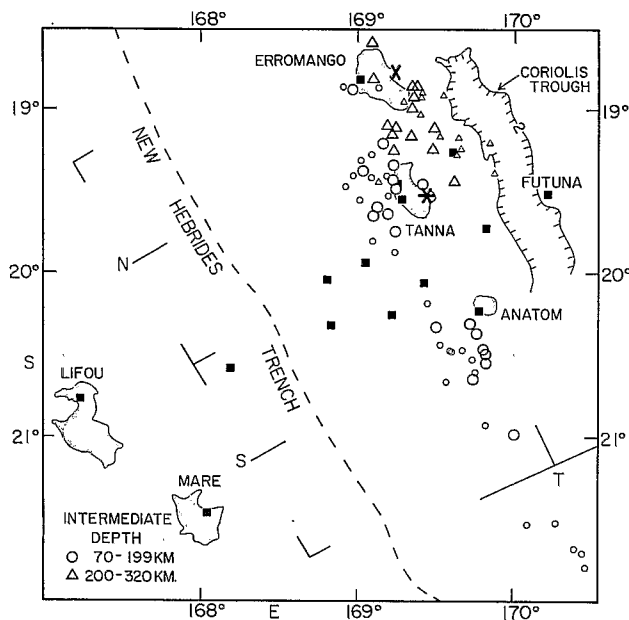
Fig. 16. Map showing intermediate-depth activity located by the local network. The shapes of the symbols indicate the depth of the hypocenters; large triangles and circles represent A and B quality locations; small triangles and circles represent C and D quality locations. Squares represent the stations of the local network. The 2-km contour of the Coriolis Trough feature and the estimate of the trench axis (dashed line) are indicated. Limits of the cross sections of Figures 13, 17, and 19 are also shown.

at 40- to 50-km depth (beneath the surface) is not due to horizontal compression. More data would be needed to establish whether these observations are indicative of the main stress.

One of the interesting features of the northern section (Figure 13) is the location within the subducting plate of two events (d and e) with a 50-km hypocentral depth. These are good locations and give a lower limit to the thickness of the seismically active part of the subducted plate just beneath the plate boundary. The distance between these events and the estimated zone of contact between the plates is about 40 km. This observation agrees with the estimates of the seismically active thickness of subducted plates given by *Isacks and Barazangi* [1977], *Pascal et al.* [1978], *Chen and Forsyth* [1978], *Hasegawa et al.* [1978], and others. These observations have been explained in terms of bending or unbending of the descending plate [e.g., *Stauder*, 1968; *Isacks and Barazangi*, 1977; *Engdahl and Scholz*, 1977]. The two earthquakes at 50-km depth can be interpreted as being produced by stress in the lower parts of the plate as it bends. It may be related either to downdip compression due to the downward bending of the plate or to horizontal extension due to the lateral bending of the plate, as indicated by the curvature of the trench in the southern New Hebrides arc. Though the first-motion data recorded by the local stations do not yield a unique focal mechanism, they are consistent with the bending hypothesis (d and e, Figure 15).

Shallow activity within the suboceanic plate but located to the west of the trench axis was also recorded during the experiment and includes primarily the August 16 event ($Ms = 4.9$) and its aftershocks (see Figure 10). These events are too far from the network to have well-constrained depths. However, the origin time of the mainshock was estimated from the S and P arrival times recorded at the local stations and plotted on a Wadati diagram. Different locations of the mainshock were then obtained with all available P wave (teleseismic and
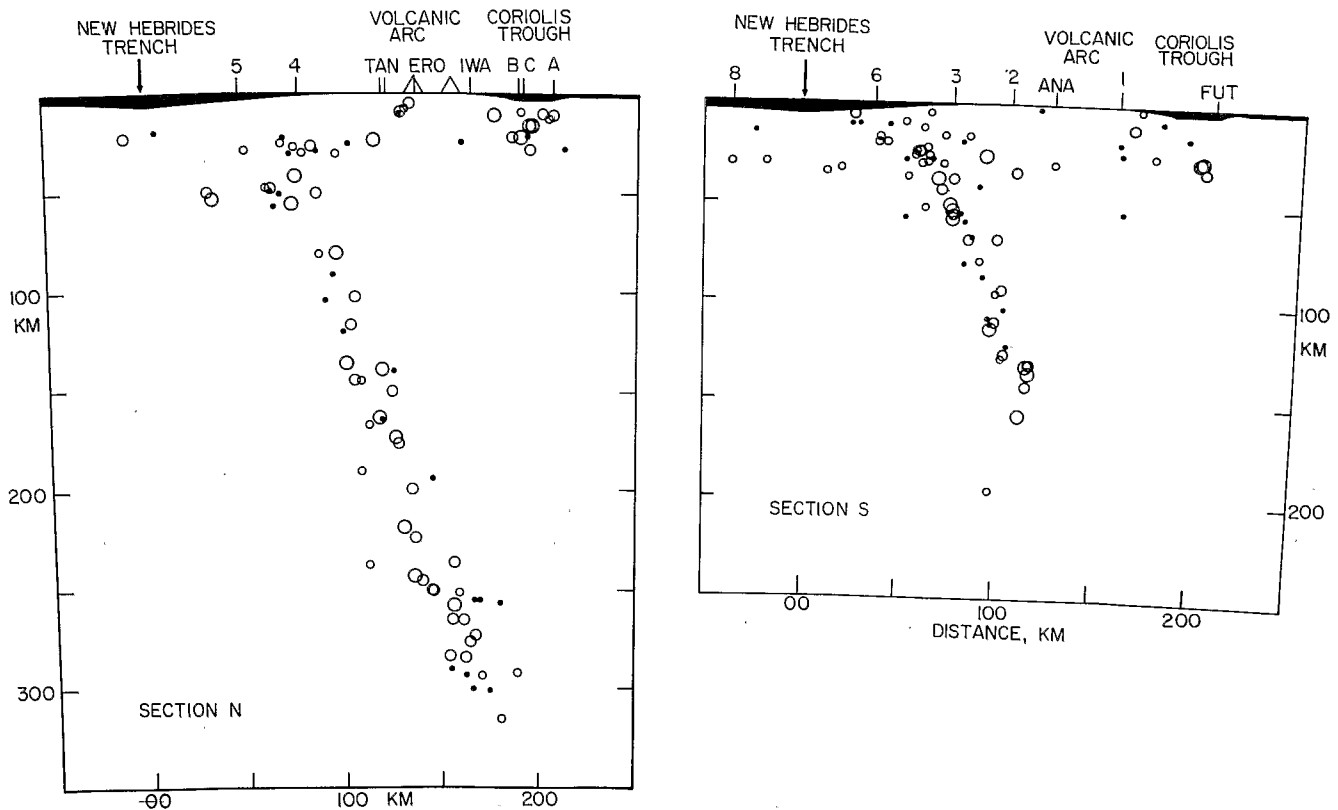

Fig. 17. The activity located by the local network projected on two cross sections that have an azimuth of N60°E. The limits of the sections are shown on Figure 16. The size of the symbols decreases with the quality of the location. Quaternary volcanoes are indicated on the zero depth line by triangles. For clarity, the two swarms of shallow events located near 19°S on Figure 10 have not been shown.
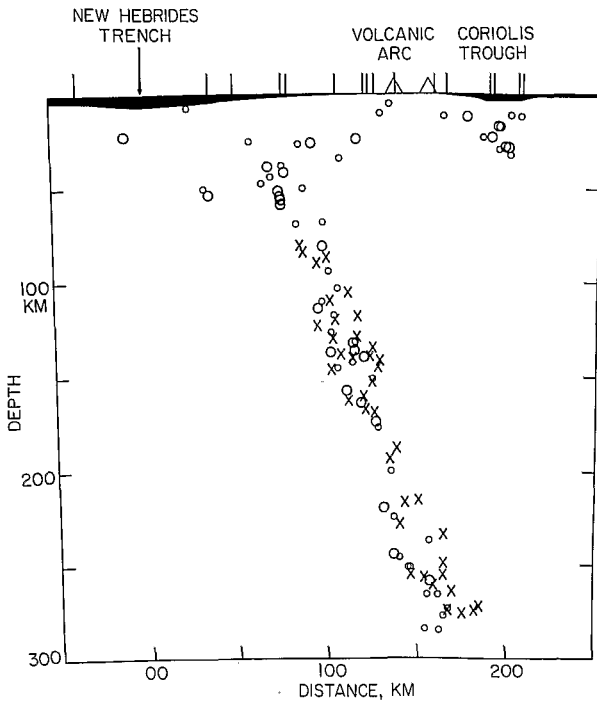
Fig. 18. Cross section directed N60°E showing the geometry of the Benioff zone in southern New Hebrides. The limits of the section are represented by the outer limits of sections N and S of Figure 16. The circles indicate all the A and B quality locations determined by the local network; the crosses represent the events located by the ISC with more than 35 stations during the period between 1964–1977.

local) data but with the focal depth constrained in each case. The best agreement with the locally determined origin time was for a depth constrained at 20 km. This result is in good agreement with the range of depths of the large normal faulting earthquakes that are located in the suboceanic plates near the trench, as reported by *Chapple and Forsyth* [1979].

Two Aftershock Zones North of the Network

On July 10, slightly more than 1 month before the occurrence of the August 16 earthquake located beneath the trench, a shallow event ($Ms = 5.5$) occurred in the forearc region just to the east (about 50 km) of the August 16 event (Figure 10). The sites of these two earthquakes have been particularly active during the past 17 years (Figure 11). The activity in these two "nests" is persistent and does not represent only a single swarm or aftershock sequence. Two events of the cluster in the forearc area were large enough to have their focal mechanisms and depths resolved fairly accurately. One (event 73, Figure 12) was located by D. Chinn and B. Isacks (manuscript in preparation, 1981) at 39-km depth and has a thrust-type focal mechanism interpreted as an interplate event. The other event (event 26) has a depth of 20 km and a predominantly normal faulting mechanism with one nearly vertical nodal plane. This event appears to be located in the upper plate.

These two adjacent areas of concentrated shallow activity occur in an area of complex bathymetry of the forearc [*Daniel*, 1978] and might reflect heterogeneities in structure and stress distribution. This may also be reflected by (1) the location of the productive volcanic centers which presumably built Erromango and (2) the persistently high rate of intermediate seismicity beneath Erromango. These features are located within a part of the plate boundary (between 18°S and 20°S) that has not experienced major rupture during at least the past 30 years and possibly the past 100 years [*McCann*, 1980]. Except

for the two clusters of activity, this part of the plate boundary has also been very quiet in terms of moderate size events during about the past 20 years. These results could be taken to indicate that the region is in a period of quiescence preceding a great earthquake. The close spatial association of interplate and intraplate events in the cluster suggests a stress concentration along the plate boundary and may correspond to a zone of rupture nucleation (event 73) and not a barrier to rupture propagation. Similar features are found in the central New Hebrides [*Isacks et al.*, 1981].

Shallow Seismic Activity in the Upper Plate

The four focal mechanisms of large events that occurred in the upper plate (events 26, 76, 77, and 78; Figure 12) all have a component of normal faulting, although three have one of the nodal planes oriented nearly vertically. The nearly vertical nodal planes have a NW to WNW strike in each case. If these planes are the fault planes, mainly vertical block movements are implied. This interpretation agrees with geological evidence for block movements on Erromango Island [*Colley and Ash*, 1971] and elsewhere in the New Hebrides [see, e.g., *Taylor et al.*, 1980]. Colley and Ash reported two major trends of nearly perpendicular faulting. One is well-defined around N50°W; this direction is similar to the strike of the vertical planes of the focal mechanisms. All the observed faults are nearly vertical normal faults and show uplift of the island as a series of blocks. In the same way, NW-SE trending fault scarps have imposed a differential component on the general uplift of Aniwa [*Carney*, 1977] and Tanna [*Carney and MacFarlane*, 1977]. Thus focal mechanisms as well as geologic observations indicate that the upper plate in the region of Erromango and Tanna is cut into a series of blocks that are differentially uplifted along faults with a mainly NW-SE strike.

At depths less than 35 km, several events recorded by the 1977 network and located between Tanna and Anatom seem associated with the upper plate (Figures 10 and 13). Among the numerous events associated with the volcanic activity at Tanna, several events were located with depths around 10 km (Figures 13 and 14). Small-magnitude events very close to the Anatom station were recorded (Figure 14). Note that the area near Anatom where the three larger, upper plate events occurred (events 76–78 in 1973, 1974, and 1976; Figure 12) was relatively quiet during the 1977 experiment. In contrast to the activity of moderately large events shown in Figure 12 and suggested in the PDE data shown in Figure 11, the small 1977 events located (Figure 10) show concentrations of upper plate activity beneath and near the Coriolis trough.

The Coriolis trough is part of a series of riftlike features located east of the volcanic arc in the southern and northern parts of the New Hebrides arc [*Dubois et al.*, 1978]. The narrow trough, about 2 km deep, trends approximately parallel to the arc and is located about 50 km east of the volcanic arc. During the 1977 experiment, three OBS stations (A, B, and C; Figure 2) operated for 24 hours on August 28 in the trough near Aniwa in a tripartite array with a spacing of about 20 km. The nearby station on Aniwa (IWA) operated with both continuous and event recording systems during this period. The seven well-located events recorded by this array are shown in Figure 10. Accurate depths of the five events located beneath the trough are 11, 12, 16, 22, and 22 km. These depths seem significantly greater than the depths observed beneath oceanic spreading centers. For example, *Lilwall et al.* [1978] report depths of mainly 7 km and always less than 11 km beneath the Mid-Atlantic Ridge. Thus the depths of the earth-
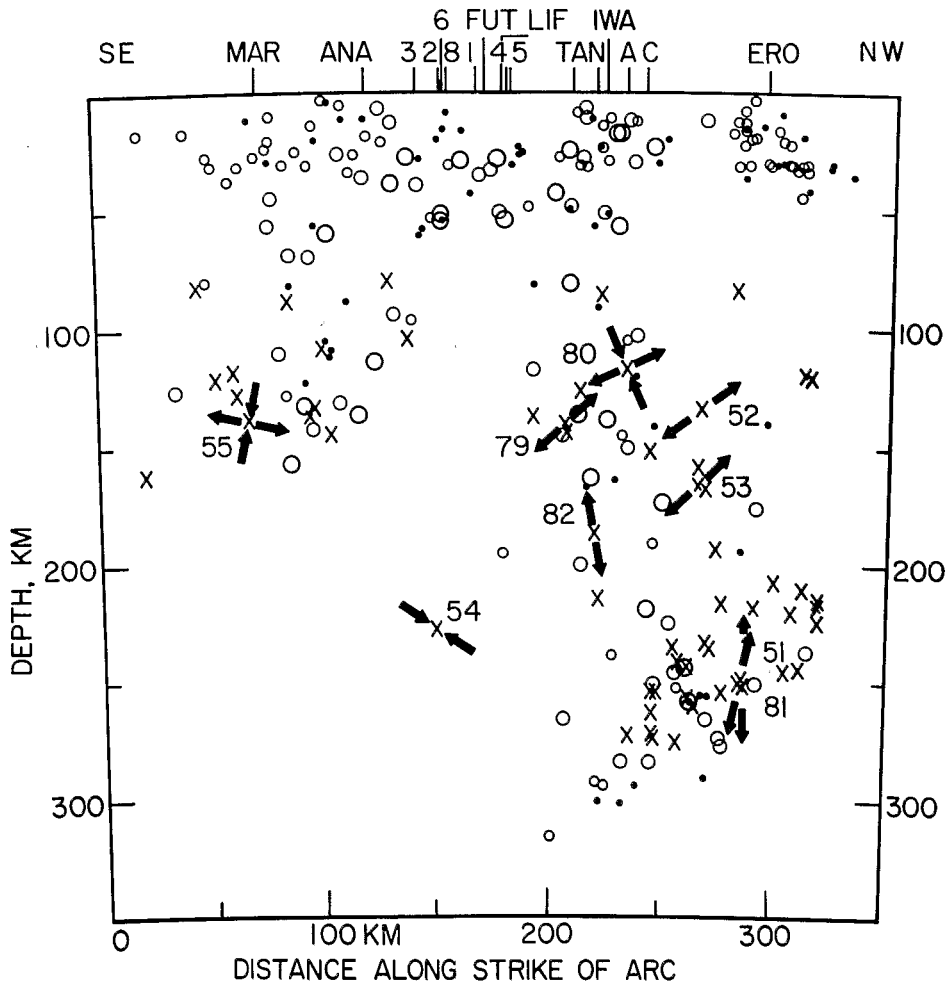
Fig. 19. The activity projected on a cross section parallel to the trench (N25°W). The circles indicate the events located by the local network; the size decreases with the quality of the locations. The crosses represent the events located by the ISC with more than 35 stations during the 1964–1977 period. The arrows show the principal axes of the stress in the subducting slab obtained from focal mechanisms of large-magnitude events located by the worldwide network. The parameters of these focal mechanisms are given in Table 4 under the reference numbers indicated on this figure.

quakes as well as the morphology of the trough suggest that the Coriolis trough is more like a continental rift zone than an actively spreading oceanic ridge. Moreover, no evidence of an anomalously thin crust localized beneath the rift was found from refraction studies [Ibrahim et al., 1980] or gravity studies [Collot et al., 1980; Oustlant, 1980; J. Y. Collot and A. Malahoff, manuscript in preparation, 1981]. The estimate of the Moho discontinuity deduced from these studies is shown in Figure 23. Though high magnetic anomalies are associated with the trough [Dubois et al., 1978], study of wave propagation to the land stations of the 1977 network shows that there is no large zone of shear wave attenuation at shallow depths beneath the trough [Isacks et al., 1978].

The question remains as to what extent the Coriolis trough is a very young feature associated with the present subducting regime [Dubois et al., 1978] or a feature originating in the late Miocene reversal of arc polarity and associated with the back arc spreading that led to the development of the Fiji Plateau. In the second case, the riftlike feature of the back arc area may be comparable to a continental margin. The main focus of the seafloor spreading is now probably located several hundred kilometers to the east [e.g., Falvey, 1975]. The shallow seismicity associated with the back arc rifts may be evidence of reactivation of the rift under the current stress regime of the subducting zone.

GEOMETRY OF BENIOFF ZONE AND MECHANISMS
OF INTERMEDIATE-DEPTH EARTHQUAKES

The intermediate-depth events located by the local network are not distributed regularly in space (Figure 16). Near Erromango most of the events are at depths greater than 200 km, whereas near Tanna the activity is spread out between depths of 70 to 300 km. No intermediate-depth activity was recorded between Tanna and Anatom. South of Anatom, no events at depths greater than 175 km were located. This uneven distribution makes determinations of the geometry of the Benioff zone difficult.

Pascal et al. [1978] showed that the overall distribution of intermediate-depth events along much of the New Hebrides arc is well represented by an inclined slab with a strike of N20°W and a dip of 70°. Pascal et al.'s section ended near Tanna. South of Erromango, the N20°W direction does not fit the strike of the Benioff zone defined in map view by the events at similar depths (Figure 16). The trench in this part of the New Hebrides is slightly arcuate (Figure 1) and can be approximated from 19°S to 21°S by a line striking N30°W. This trend was chosen as the direction of the strike of the inclined zone. In Figure 17 the hypocenters are projected onto two vertical sections directed perpendicular to the strike. The two sections do not present any significant difference in the shape of
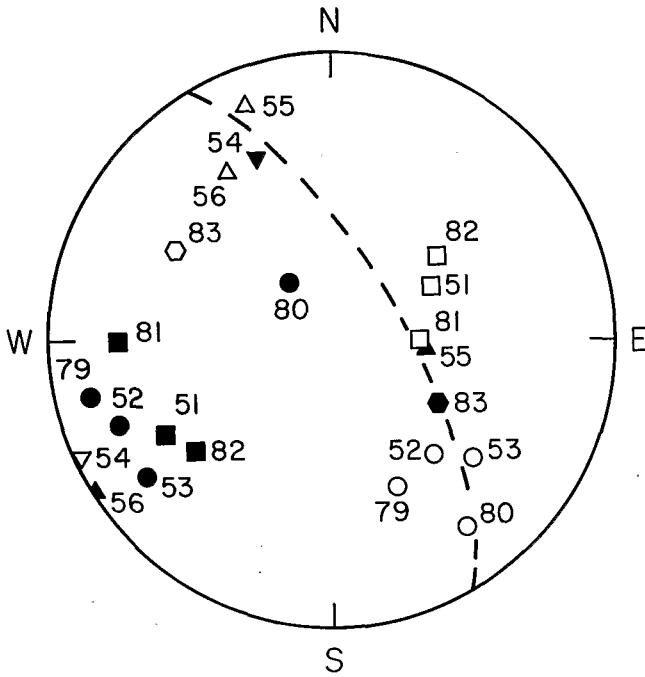
Fig. 20. Summary of the known focal mechanisms of large-magnitude intermediate-depth events located in the southern New Hebrides. The P axes (solid symbols) and T axes (open symbols) are plotted on equal area projection of the lower hemisphere of a common focal sphere. The dashed line indicates the trace of the Benioff zone. The focal mechanisms are numbered as in Table 4 and Figure 19. The different symbols refer to different sets of earthquakes, as discussed in the text.

the Benioff zone. All the well-located events (A and B quality) projected onto the same section define a 20-km-thick Benioff zone with a 70° dip (Figure 18). These results are in good agreement with the general shape of the Benioff zone in the New Hebrides [Isacks and Barazangi, 1977; Pascal et al., 1978].

Figure 18 also shows the intermediate-depth events located by the ISC with at least 35 P readings for the period 1964–1977. The agreement between the two sets of locations is very good for depths between 70 and 200 km. The slight difference suggested at larger depths is probably due to mislocation by the local network, as discussed in a previous section. The ISC events shown in Figure 18 are located in the region from south of Anatom to south of Erromango. If events located beneath and somewhat north of Erromango were included, the Benioff zone would be wider. This indicates a misprojection of the activity and is in accordance with the result that near Erromango the strike of the Benioff zone is closer to N20°W than to N30°W. It is beyond the resolution of the data to determine whether this change of trend occurs as a discontinuity in the shape of the slab or as a progressive lateral bending of the Benioff zone as suggested by the shape of the trench axis.

A progressive bending of the Benioff zone is favored by interpretation of the focal mechanism solutions of intermediate-depth events. The stress axes (P and T axes) determined by the focal mechanism solutions of events large enough to be well recorded by the long-period seismographs of the WWSSN (see Tables 4 and 5, and Figure 22) are shown in Figure 19 on a front view (i.e., longitudinal section) of the Benioff zone. All the focal mechanisms have at least one of the stress axes in or near the plane of the Benioff zone (Figure 20), and though in Figure 19 the section is vertical, it is the stress axis within the plane dipping 70° that is shown. The

stresses in the subducting plate show a complex variation with depth and location. North of Tanna, between 100 and 175 km depth (events 52, 53, 79, and 80) the T axes have both a downdip and a lateral component (inclined downward toward the south) (circles in Figure 20). These mechanisms can be interpreted as the superposition of a downdip extensional stress and a lateral extensional stress. At depths greater than 175 km, the three events north of Tanna (events 51, 81, and 82) have focal mechanisms resulting from predominantly downdip extensional stress (squares in Figure 20). This is the general pattern of the intermediate-depth activity in the northern and central New Hebrides [Isacks and Molnar, 1971].

Between Anatom and Tanna, one earthquake (event 54) shows a pattern of compression in the plane of the slab with a large lateral component. This earthquake is located in a remarkably quiet part of the Benioff zone. Very little activity has been recorded between Anatom and Tanna since 1961 (see Figures 19 and 21). Moreover, it is the only earthquake deeper than 175 km recorded south of 19.5°S. It is conceivable (but speculative) to interpret this mechanism as a lateral compression effect on the opposite side of the descending plate from the other events (note, for example, in Figure 20, the nearly exact opposite pattern of stress of focal mechanisms for events 54 and 56).

The focal mechanism solutions of two of the events south of Anatom (event 55, Figure 19; event 56, Table 4) have their T axes oriented nearly horizontally (triangles in Figure 20); however, event 55 also has a downdip P axis. Located farther south and at shallower depth (72 km), event 83 (Table 4 and Figures 20 and 22) also shows a mechanism of downdip compression with a lateral component.

Although the pattern of stresses shown in Figures 19 and 20 is complex, all except one of the events at depths greater than 100 km have a T axis within the dipping plate. This suggest a predominance of extensional stress with downdip as well as horizontal components. Horizontal components of stress are related to a lateral bending of the Benioff zone [e.g., Isacks and Molnar, 1971; Cardwell and Isacks, 1978]. If plate bending
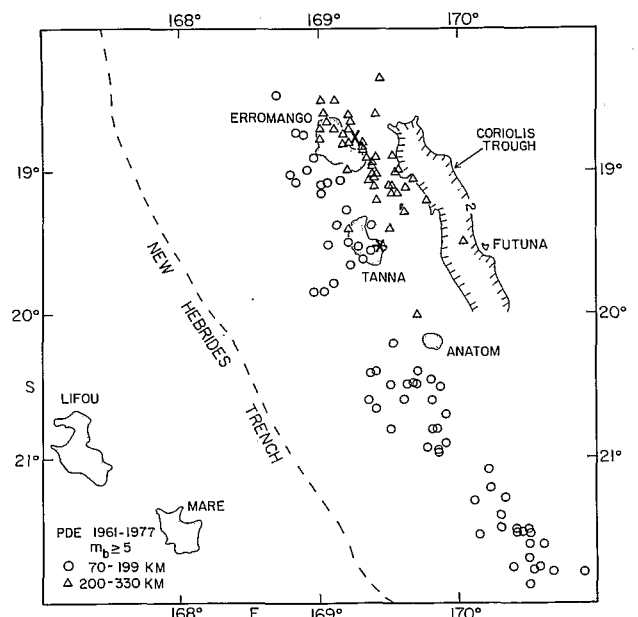

Fig. 21. Position of the intermediate-depth events of $Mb \geq 5$ between 1961 and 1977. The 2-km contour of the Coriolis Trough feature and the estimate of the trench axis (dashed line) are indicated.
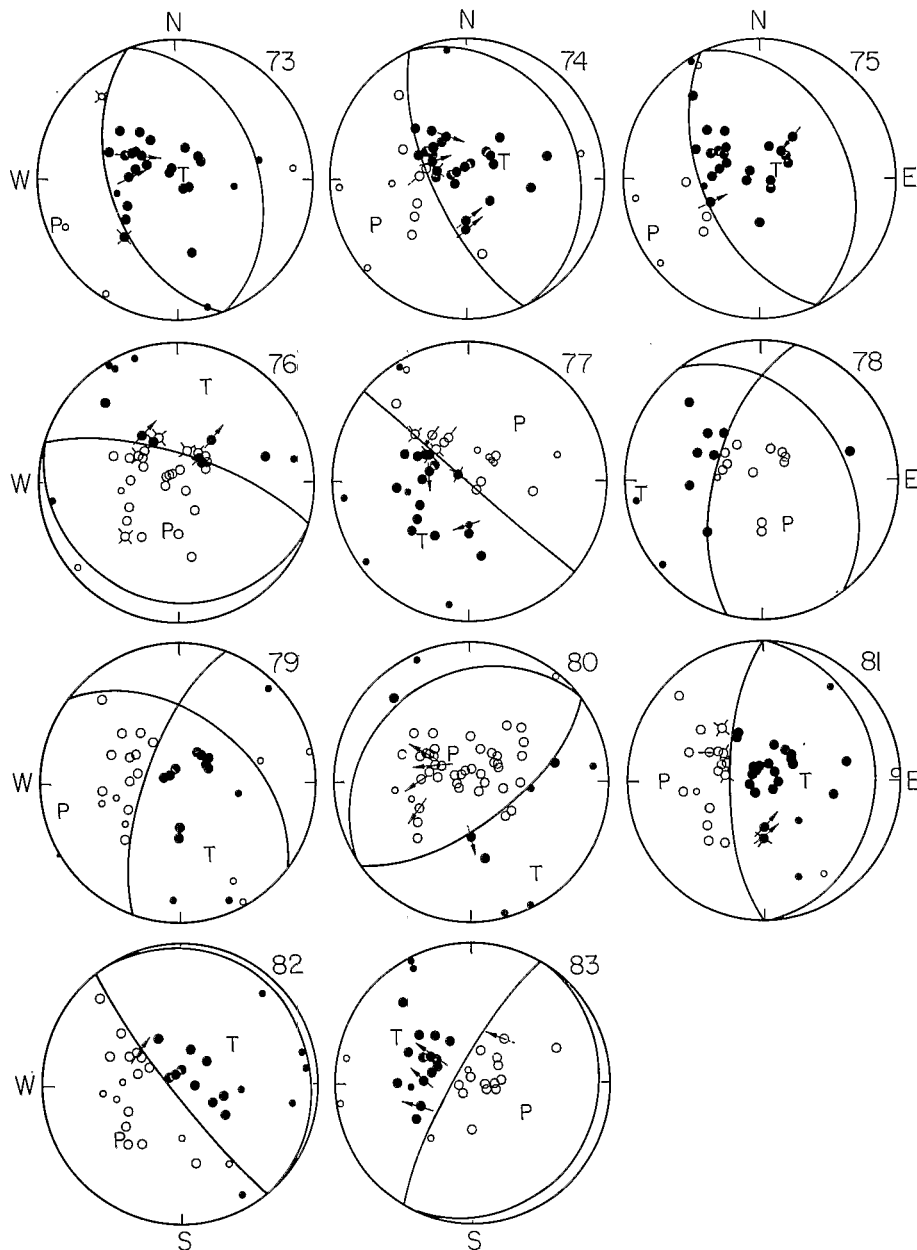
Fig. 22. New focal mechanism solutions illustrated on equal area projections of the lower hemisphere of the focal sphere. Solid circles indicate compressional first motions; open circles indicate dilatational first motions. Smaller symbols represent less reliable determinations of the first motions. Crosses indicate data judged to be near a nodal plane. The direction of first motion of S is shown by an arrow. P and T represent the axis of compression and the axis of tension, respectively. The parameters of the solutions are presented in Table 5.

effects are important, then mechanisms such as that for event 54, which has reversed polarities, migh be expected on the opposite side of the bending plate.

Though the intermediate-depth activity located during a 4-week period is a short sample of the seismicity of the region, the pattern of the spatial distribution of the located earthquakes is remarkably similar to that obtained by the ISC or PDE for a 17-year period (see Figures 10, 11, 16, and 21). This similarity implies that over a 17-year time scale the seismicity occurs persistently in specific places in the arc and includes a large range of magnitudes. As Santo [1970] and others have described, persistent nests of activity characterize the intermediate-depth seismicity in numerous areas. Either these features slowly change over time scales longer than 17 years, or these represent features of the structure or geometry of the

subducting plate. Pascal et al. [1978] showed that a prominent nest in the central New Hebrides is probably associated with the subducted portion of the d'Entrecasteaux fracture zone [see also Chung and Kanamori, 1978]. The aligment of the shallow nests of activity west of Erromango and the intermediate-depth nest beneath Erromango suggest structural control of these features as well, although there is no direct evidence for this in the bathymetry of the seaward part of the oceanic plate.

CONCLUSIONS

The following are the main conclusions of this study:
1. We observed strikingly small differences (less than about 10 km) in the locations of shallow- and intermediate-depth earthquakes located by the temporary local network
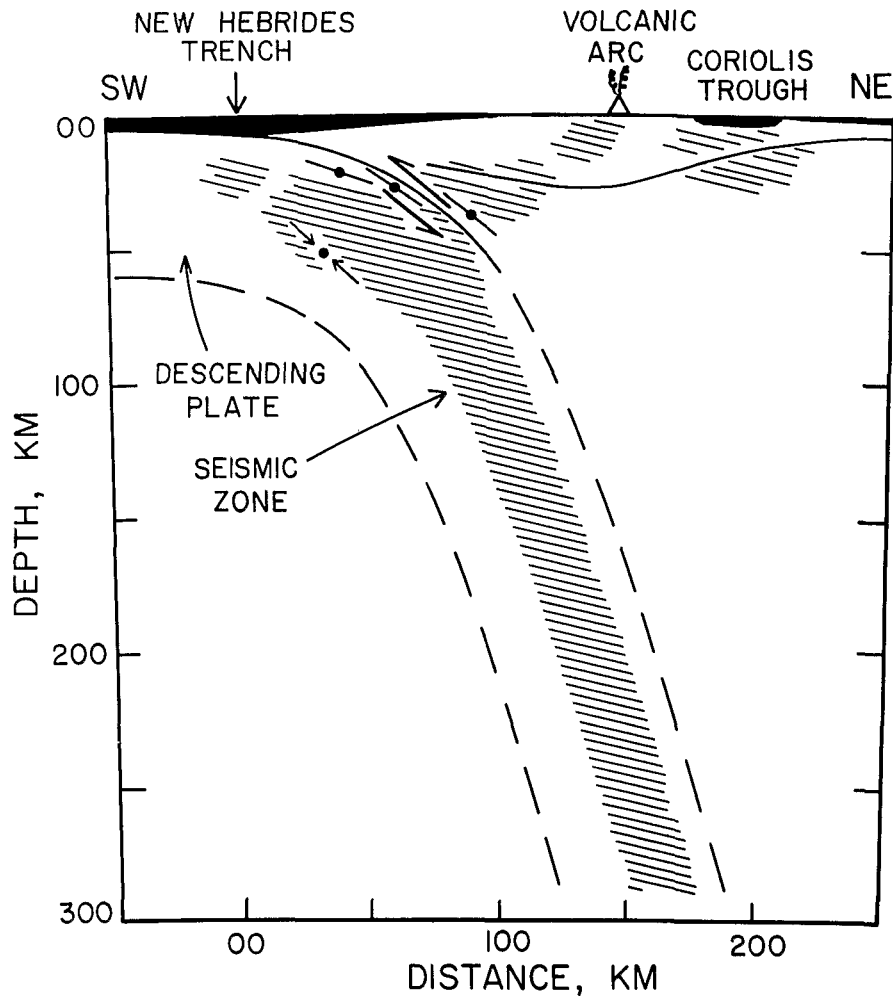
Fig. 23. A schematic cross section showing the region where shallow and intermediate-depth earthquakes were recorded (inclined lines) and the inferred geometry of the descending plate beneath the southern New Hebrides arc. The inferred geometry of the interplate thrust zone is partly based on the slip vectors (short, solid lines) of the shallow thrust-type focal mechanisms. The Moho discontinuity of the overriding plate estimated from refraction and gravity studies is also shown.

and by the ISC using worldwide stations. These results are in marked contrast to those obtained from many other arcs and probably are partly caused by the very wide aperture of the local network and by the unique geometry of the subduction system, which includes a very narrow arc and a steeply dipping Benioff zone. We did, however, find evidence of a high-velocity zone (at least 5% higher than the surrounding mantle) associated with the subducting plate.

2. The pattern of the spatial distribution of shallow- and intermediate-depth earthquakes as determined by the short-duration temporary network is remarkably similar to that obtained (excluding aftershocks) by the PDE or by the ISC for about a 20-year period.

3. The small events located in this study poorly define the interplate thrust zone that exists between the descending and overriding plates. The thrust zone is mainly defined by the spatial distribution and mechanisms of moderate to large size events and their aftershocks. A striking observation is the narrow width (about 60 km) of the New Hebrides plate boundary as defined by the interplate thrust zone (Figure 23).

4. Considerable shallow seismic activity occurs within the suboceanic descending plate beneath the trench and beneath the interplate thrust zone (Figure 23). The spatial distribution

of this activity gives a lower limit of about 40 km to the thickness of the seismically active part of the descending plate just beneath the interplate thrust zone. The focal mechanisms of some of these events can be interpreted as a consequence of bending effects of the descending plate.

5. Most focal mechanisms of moderate to large size earthquakes that occurred within the upper plate have a component of normal faulting with one of the nodal planes oriented nearly vertically. These mechanisms and geological observations on the islands suggest that the upper plate in the region of Erromango and Tanna is divided into a series of blocks that are differentially uplifted along mainly NW-SE striking faults.

The small events that are well-located in the upper plate during the 1977 experiment show concentrations of activity beneath the Coriolis trough (Figure 23). This trough is part of a series of riftlike features located to the east of the volcanic arc. The depths of these events (as deep as 22 km) as well as the morphology of the trough suggest that the Coriolis trough is more like a continental rift than an oceanic-type rift zone.

6. The distribution of intermediate-depth events is clustered in space. All the well-located events define a 20-km thick Benioff zone that has a dip of about 70° (Figure 23).

The focal mechanisms of moderate to large size, intermediate-depth events are best interpreted as due to effects of downdip extension and lateral bending (or unbending) in the descending plate near the southern end of the New Hebrides arc.

REFERENCES

Barazangi, M., and B. Isacks, A comparison of spatial distribution of mantle earthquakes determined from data produced by local and by teleseismic networks for the Japan and Aleutian arcs, *Bull. Seismol. Soc. Am., 69,* 1763–1770, 1979.

Buland, R., The mechanics of locating earthquakes, *Bull. Seismol. Soc. Am., 66,* 173–187, 1976.

Cardwell, R., and B. Isacks, Geometry of the subducted lithosphere beneath the Banda Sea in eastern Indonesia from seismicity and fault plane solutions, *J. Geophys. Res., 83,* 2825–2838, 1978.

Carney, J. N., Aniwa, *Annu. Rep. Geol. Surv. New Hebrides 1975,* 40 pp., 1977.

Carney, J. N., and A. MacFarlane, Tanna, *Annu. Rep. Geol. Surv. New Hebrides, 1975,* 40 pp., 1977.

Carney, J. N., and A. MacFarlane, Lower to middle Miocene sediments on Maewo, New Hebrides and their relevance to the development of the outer Melanesian arc system, *Bull. 9,* p. 3, Aust. Soc. Explor. Geophys., Sydney, 1978.

Chapple, W., and D. Forsyth, Earthquakes and bending of plates at trenches, *J. Geophys. Res., 84,* 6729–6749, 1979.

Chase, C. G., Tectonic history of the Fiji Plateau, *Geol. Soc. Am. Bull., 82,* 3087–3110, 1971.

Chatelain, J. L., S. Roeker, D. Hatzfeld, and P. Molnar, Microearthquake sesmicity and fault plane solutions in the Hindu Kush region and their tectonic implication, *J. Geophys. Res., 85,* 1365–1387, 1980.

Chen, T., and D. Forsyth, A detailed study of two earthquakes seaward of the Tonga Trench, *J. Geophys. Res., 83,* 4995–5003, 1978.

Chung, W. Y., and H. Kanamori, Subduction process of a fracture zone and aseismic ridges: The focal mechanism and source characteristics of the New Hebrides earthquake of 1969 January 19 and some related events, *Geophys. J. R. Astron. Soc., 54,* 221–240, 1978.

Colley, H., and R. Ash, The geology of Erromango, regional report, 112 pp., New Hebrides Geol. Surv., Vila, 1971.

Collot, J. Y., and F. Missegue, Crustal structure between New Caledonia and New Hebrides, in *Geodynamics in South West Pacific,* pp. 135–144, Editions Technip, Paris, 1977.

Collot, J. Y., J. Daniel, R. Louat, P. Maillet, B. Pontoise, B. Isacks, G. Latham, and A. Malahoff, La zone de subduction des Nouvelles Hebrides, *Congr. Geol. Int., 26th,* 1980.

Coudert, E., Etude de la sismicite du Sud de l'arc insulaire des Nouvelles Hebrides, enregistree par un reseau temporaire de stations locales terrestres et sous-marines, these de doctorat de 3eme cycle, Univ. de Paris-SUD, Paris, 1980.

Daniel, J., Morphology and structure of the southern part of the New Hebrides island arc system, *J. Phys. Earth, 26,* S181–S190, 1978.

Davies, J., and L. House, Aleutian subduction zone seismicity, volcano-trench separation, and their relation to great thrust-type earthquakes, *J. Geophys. Res., 84,* 4583–4591, 1979.

Dubois, J., Contribution a l'etude structurale du Sud-Ouest Pacifique d'apres les ondes sismiques observees en Nouvelle Caledonie et aux Nouvelles Hebrides, these de doctorat es Sciences Physiques, 160 pp., Univ. de Paris, Paris, 1969.

Dubois, J., Propagation of P Waves and Rayleigh waves in Melanesia: Structural implications, *J. Geophys. Res., 76,* 7217–7240, 1971.

Dubois, J., F. Dugas, A. Lapouille, and R. Louat, The troughs at the rear of the New Hebrides island arc: Possible mechanisms of formation, *Can. J. Earth Sci., 15,* 351–360, 1978.

Engdahl, E., and C. Scholz, A double Benioff zone beneath the central Aleutians: An unbending of the lithosphere, *Geophys. Res. Lett., 4,* (10), 473–476, 1977.

Engdahl, E., N. Sleep, and M. T. Lin, Plate effects in North Pacific subduction zones, *Tectonophysics, 37,* 95–116, 1977.

Falvey, D., Arc reversals and a tectonic model for the North Fiji Basin, *Bull., 6,* pp. 47–49, Aust. Soc. Explor. Geophys., Sydney, 1975.

Gill, J., and M. Gorton, A proposed geological and geochemical history of Eastern Melanesia, in *The Western Pacific: Island Arcs, Marginal Seas, Geochemistry,* edited by P. J. Coleman, pp. 543–566, University of Western Australia Press, Nedlands, 1973.

Hasegawa, A., N. Umino, and A. Takagi, Double planed deep seismic zone and upper mantle structure in the northeastern Japan arc, *Geophys. J. R. Astron. Soc., 54,* 281–296, 1978.

Ibrahim, A., and G. Latham, A comparison between sonobuoy and ocean bottom seismograph data and crustal structure of the Texas shelf zone, *Geophysics, 43,* 514–527, 1978.

Ibrahim, A., B. Pontoise, G. Latham, B. Larue, T. Chen, B. Isacks, J. Recy, and R. Louat, Structure of the New Hebrides Arc–Trench system, *J. Geophys. Res., 85,* 253–266, 1980.

Isacks, B., and M. Barazangi, Geometry of Benioff zones: Lateral segmentation and downward bending of the subducted lithosphere, in *Island Arcs, Deep Sea Trenchs and Back-Arc Basins, Maurice Ewing Ser.,* vol. 1, edited by M. Talwani and W. Pitman, pp. 99–114, AGU, Washington, D. C., 1977.

Isacks, B., and P. Molnar, Distribution of stresses in the descending lithosphere from a global survey of focal mechanism solutions of mantle earthquakes, *Rev. Geophys. Space Phys., 9,* 103–174, 1971.

Isacks B., E. Coudert, R. Cardwell, M. Barazangi, L. Louat, G. Latham, A. Chen, and J. Dubois, Results from a land-OBS seismograph network temporarily deployed across the southern New Hebrides island arc, *Earthquake Notes, 49,* 29–30, 1978.

Isacks, B. L., R. Cardwell, J.-L. Chatelain, M. Barazangi, J.-M. Marthelot, D. Chinn, and R. Louat, Seismicity and tectonics of the central New Hebrides Island Arc, in *Earthquake Prediction, Maurice Ewing Ser.,* vol. 4, edited by D. W. Simpson and P. G. Richards, in press, AGU, Washington, D. C., 1981.

James, D., S. Sacks, E. Lazo, and P. Aparicio, On locating local earthquakes using small networks, *Bull. Seismol. Soc. Am., 59,* 1201–1212, 1969.

Johnson, T., and P. Molnar, Focal mechanisms and plate tectonics of southwest Pacific, *J. Geophys. Res., 77,* 5000–5032, 1972.

Kaila, K., and V. Krishna, Upper mantle velocity structure in the New Hebrides island arc region, *J. Phys. Earth, 26,* S139–S153, 1978.

Karig, D., and J. Mammerickx, Tectonic framework of the New Hebrides island arc, *Mar. Geol., 12,* 87–205, 1972.

Lee, W., and J. Lahr, HYPO 71 (revised): A computer program for determining hypocenter, magnitude, and first motion pattern of local earthquakes, *Geol. Surv. Open File Rep. U.S., 75-311,* 114 pp., 1975.

Lilwall, R., and T. Francis, Hypocentral resolution of small ocean bottom seismic networks, *Geophys. J. R. Astron. Soc., 54,* 721–728, 1978.

Lilwall, R., T. Francis, and I. Porter, Ocean bottom seismograph observations on the mid-Atlantic Ridge near 45 N: Further results, *Geophys. J. R. Astron. Soc., 55,* 255–262, 1978.

Louat, R., J. Dubois, and B. Isacks, Evidence for anomalous propagation of seismic waves within the shallow zone of shearing between the converging plates of the New Hebrides subduction zone, *Nature, 281,* 293–295, 1979.

Mallick, D., Development of the New Hebrides Archipelago, *Philos. Trans. R. Soc. London, 272,* 277–285, 1975.

Mammerickx, J., T. Chase, S. Smith, and I. Taylor, Bathymetry of the South Pacific, map, Scripps Inst. of Oceanogr., LaJolla, Calif., 1971.

McCann, W., Seismic potential and seismic regimes of the southwest Pacific, submitted to *J. Geophys. Res.,* 1980.

Mitronovas, W., and B. Isacks, Seismic velocity anomalies in the upper mantle beneath the Tonga-Kermadec island arc, *J. Geophys. Res., 76,* 7154–7180, 1971.

Oustlant, J.-L, Modelisation a partir des donnees marines de sismique refraction et de gravimetrie: Application a quelques exemples dans

le Sud Ouest Pacifique, these de doctorat de 3eme cycle, Univ. Paris 6, Paris, 1980.

Pascal, G., B. Isacks, M. Barazangi, and J. Dubois, Precise relocation of earthquakes and seismotectonics of the New Hebrides island arc, *J. Geophys. Res., 83,* 4957–4973, 1978.

Peter, D., and R. Crosson, Application of prediction analysis to hypocenter determination using local array, *Bull. Seismol. Soc. Am., 62,* 775–788, 1972.

Santo, T., Regional study on the characteristic seismicity of the world, Part III, New Hebrides island region, *Bull. Earthquake Res. Inst. Tokyo Univ., 48,* 1–18, 1970.

Stauder, W., Tensional character of earthquake foci beneath the Aleutian trench with relation to sea floor spreading, *J. Geophys. Res., 73,* 7693–7701, 1968.

Suyehiro, K., and I. Sacks, P and S wave velocity anomalies associated with the subducting lithosphere determined from travel time residuals in the Japan region, *Bull. Seismol. Soc. Am., 69,* 97–115, 1979.

Taylor, F., B. Isacks, C. Jouannic, A. Bloom, and J. Dubois, Coseismic and Quaternary vertical tectonic movements, Santo and Malekula islands, New Hebrides island arc, *J. Geophys. Res., 85,* 5367–5381, 1980.

Utsu, T., Regional variation of travel time residuals of P-waves from nearby deep earthquakes in Japan and vicinity, *J. Phys. Earth, 23,* 367–380, 1975.

Ward, P. L., G. Palmason, and C. Drake, Microearthquake survey and the mid-Atlantic ridge in Iceland, *J. Geophys. Res., 74,* 665–684, 1969.